UNIVERSITÀ
DEGLI STUDI
DI PADOVA

UNIVERSITÀ DEGLI STUDI DI PADOVA

DIPARTIMENTO DI MEDICINA MOLECOLARE

Scuola di Dottorato di Ricerca in Biomedicina

CICLO XXVII

Human red blood cells alterations in Primary Aldosteronism: Mineralocorticoid Receptor (MR) involvement in the Aldosterone pathway

Direttore della Scuola: Ch.mo Prof. Riccardo Manganelli

Supervisore: Prof. Giulio Clari

Ch.mo Prof. Fulvio Ursini *

Dottorando: **Dr. Gabriella Donà**

*** Il Prof. Fulvio Ursini è subentrato come supervisore in seguito alla scomparsa del Prof. Giulio Clari.**

Il mio lavoro di tesi è stato seguito principalmente nella sua parte sperimentale dal Prof. Clari e dalla Dott.ssa Luciana Bordin, in collaborazione con il Prof. Decio Armanini.

Al Prof. Giulio Clari

CONTENTS

ABBREVIATIONS

Ab	Antibody
Aldo	Aldosterone
BSA	Bovine serum albumin
CA	Carbonic anhydrase
Can	Canrenone
Cort	Cortisol
DTT	Dithiothreithol
Gelda	Geldanamycin
G6PDH	Glucose-6-phosphate dehydrogenase
GSH	Reduced glutathione
GSSP	Glutathione-protein mixed disulphide
Hb	Hemoglobin
HMWA	High molecular weight aggregates
HRP	Horse radish peroxidase
IgG	Immunoglobulin G
MR	Mineralocorticoid receptor
OS	Oxidative stress
PA	Primary aldosteronism
PAGE	Polyacrylamide gel electrophoresis
PBS	Phosphate buffered saline
PTKs	Protein tyrosine kinases
PTPs	Protein tyrosine phosphatases
RBCs	Red blood cells
ROS	Reactive oxygen species
SDS	Sodium dodecyl sulphate
Tyr-P	Tyrosine phosphorylation
WB	Western blotting

ABSTRACT

Red blood cells (RBCs) are a-nucleated cells particularly exposed to different stimuli, among which circulating hormones and intra/extra-cellular derivatives from oxidization processes. In addition, our previous studies showed that in the case of inflammatory diseases with GSH content alterations, RBCs were much more sensitive to diamide, a mild oxidant able to trigger tyrosine-phosphorylation (Tyr-P) of membrane proteins, mainly band 3.

Aldosterone (Aldo), mineralocorticoid hormone, has been shown to induce many effects other than the common diuretic process regulation and involving the expression and activation of the superoxide generating enzyme NADPH oxidase, thus potentially explaining the increased plasma markers of oxidative stress (OS) like isoprostanes in primary aldosteronism (PA), disease characterized by excessive Aldo secretion. This well-known Aldo action is mediated by the activation of a cytosolic specific receptor, the mineralocorticoid receptor (MR), in the so called genomic pathway, which distinguishes from the direct effect of Aldo on many proteins and enzymes in the second mechanism, also known as non-genomic pathway.

Starting from these evidences, if a direct Aldo involvement in the triggering of inflammatory-related oxidative status of the cells was evolving, RBCs were the eligible cells for the investigation of the non-genomic Aldo pathway.

The study involved PA patients and healthy control (HC) and consisted with three phases: i) a first approach was carried out to evidence potential alterations in PA RBCs followed by an *in vitro* deepening to assess the effective direct/indirect involvement of Aldo in these alterations; ii) once identified as responsible of the RBCs alterations found in PA, Aldo pathway within HC RBCs cytosol was investigated; iii) at last, Aldo-related pathway in RBCs was studied with particular attention to the mechanism leading to membrane band 3 alterations starting from Aldo induced receptor activation.

In the first part, PA RBCs were showed to have oxidative-like alterations such as band 3 protein increase of both Tyr-P level and clustering, thus suggesting that PA

could be linked to other inflammatory diseases. The effects of Aldo, cortisol (Cort) and canrenone (Can) (added as agonist and inhibitor, respectively) were compared and Aldo was confirmed as the only responsible of the alterations previously observed in PA RBCs. Furthermore, Aldo was shown to trigger RBCs membrane alterations leading to autologous IgG binding in a sort of premature ageing of the cells.

The second part of the study analyzed the mechanism of Aldo action: for the first time MR was identified in RBCs cytosol as a soluble multi-protein complex, differently regulated by the effector utilized. In facts, in the presence of Aldo, MR broke away from the complex to form dimers which were promptly proteolysed in a sort of turn off signaling. Can or Cort were not able to trigger similar events, thus explaining the different alterations found on RBCs membranes.

However, since to now no direct evidence was found about the possibility that Aldo induced an increase of oxidation status in RBCs, oxidization level in both membranes and cytosol was addressed in the third and last part of the study. Results showed no difference in GSH and GSSP contents and carbonic anhydrase (CA) monomerization and activity between HC and PA RBCs. In contrast, preliminary data would confirm a sort of oxidative-related increase of band 3 disulfide bond formation, thus suggesting a new intriguing mechanism leading to band 3 increased oxidative status without changing the common anti-oxidative cellular defenses. Further investigations addressing this mechanism are in progress.

In conclusion, we found that in PA RBCs Aldo is responsible for the membrane alterations leading to a potential premature removal of the cells from circulation. Aldo exerts its effect through the activation of the soluble MR complex, which participates in the modulation of the Aldo signaling through the possibility of being differently affected by other steroids or Aldo inhibitors (Can). Further studies are in progress to explore both nature and potential mediators of the Aldo-induced alterations in the band 3 dimer formation.

RIASSUNTO

Gli eritrociti (RBCs) sono cellule non nucleate particolarmente esposte a differenti stimoli, tra i quali l'effetto degli ormoni circolanti nel sangue e i derivati dei processi di ossidazione intra o extracellulari. Studi precedenti condotti nel nostro laboratorio hanno dimostrato che, nel caso di malattie infiammatorie con alterazione del contenuto di GSH rispetto ai controlli, gli eritrociti erano molto più sensibili alla diamide, un blando ossidante in grado di innescare la tirosin-fosforilazione (Tyr-P) delle proteine di membrana, principalmente della proteina banda 3.

L'aldosterone (Aldo), ormone mineralocorticoide, oltre alla sua classica azione regolatoria dei processi diuretici, è in grado di indurre molti altri effetti tra i quali l'espressione e l'attivazione dell'enzima NADPH ossidasi, generatore di anione superossido. Questo fatto potrebbe potenzialmente spiegare l'incremento di marker plasmatici di stress ossidativo (OS) come gli isoprostani, nell'aldosteronismo primitivo (PA), patologia caratterizzata da un'eccessiva secrezione di Aldo.

Partendo da queste evidenze, gli RBCs erano cellule ottimali per studiare se l'Aldo potesse indurre un aumentato stato di ossidazione determinato da una sua azione diretta sui processi infiammatori. Infatti, in queste cellule non nucleate, un eventuale coinvolgimento dell'Aldo nei meccanismi infiammatori, mediante un'azione non-genomica, sarebbe stato univocamente dimostrato.

Lo studio ha coinvolto sia pazienti con PA che controlli sani (HC) e si è svolto in tre fasi: i) in un approccio iniziale abbiamo valutato se esistessero potenziali alterazioni negli RBCs dei pazienti, procedendo, poi, con un approfondimento *in vitro* condotto sugli RBCs di HC per confermare o meno un diretto coinvolgimento dell'Aldo nell'indurre queste alterazioni; ii) una volta identificato come responsabile effettivo delle alterazioni riscontrate, abbiamo cercato di chiarire il meccanismo di azione dell'Aldo a livello citosolico; iii) infine, partendo dall'evidenza che l'azione dell'Aldo veniva mediata dall'attivazione del recettore

citosolico, abbiamo cercato di capire il meccanismo attraverso cui questa attivazione si trasmettesse, a livello delle membrane.

Nella prima parte, abbiano dimostrato che negli RBCs dei pazienti erano presenti delle alterazioni quali un incremento sia della Tyr-P della banda 3 che una sua aggregazione, suggerendo, così, che la patologia potesse essere correlata ad uno stress ossidativo come dimostrato in altre malattie infiammatorie. Inoltre, dopo aver comparato gli effetti di Aldo, cortisolo (Cort) e canrenone (Can) (aggiunti rispettivamente come agonista ed inibitore), abbiamo confermato che era proprio l'Aldo il diretto responsabile delle alterazione che, in ultima, portavano ad un aumento della quantità degli anticorpi autologhi legati alla membrana, rispecchiando una prematuro invecchiamento cellulare.

Nella seconda parte dello studio, abbiamo dimostrato, per la prima volta, la presenza a livello citosolico del recettore dei mineralocorticoidi (MR), che risulta essere presente in un complesso multi-proteico di elevato peso molecolare. Inoltre, abbiamo evidenziato come solo l'Aldo inducesse la liberazione dell'MR dal complesso a formare dimeri prontamente proteolizzati in una sorta di spegnimento del segnale. Al contrario, né Cort né Can erano in grado di indurre l'attivazione del recettore.

Tuttavia, poiché finora non è mai stato dimostrato se l'Aldo potesse indurre un aumento delle stato ossidativo dell'eritrocita, nella terza parte dello studio abbiamo analizzato alcuni markers di ossidazione sia a livello di membrana che di citosol. I nostri risultati indicano che nessuna modifica del contenuto di GSH o di proteine glutationilate (GSSP) era presente nei pazienti rispetto ai controlli, come nessuna alterazione nella monomerizzazione e attivazione della anidrasi carbonica (CA), nuovo parametro nella valutazione di un aumentato stato di ossidazione. Tuttavia, i nostri risultati mostrano che la proteina banda 3 risulta effettivamente sottoposta ad uno stress ossidativo che ne induce l'aggregazione attraverso la formazione di ponti disolfuro. Risultato, questo, che merita ulteriori indagini ed approfondimenti.

In conclusione, abbiamo trovato che negli RBCs dei pazienti con PA l'Aldo è responsabile di alterazioni di membrana che portano ad una potenziale prematura rimozione delle cellule dalla circolazione. L'azione dell'Aldo viene mediata a

livello citosolico dall'MR, ma non dal Cort. Ulteriori studi sono in corso per esplorare sia la natura che il meccanismo di potenziali mediatori dell'effetto dell'Aldo-MR a livello delle membrane eritrocitarie.

INTRODUCTION

1. HUMAN RED BLOOD CELLS

Red blood cells (RBCs), also called erythrocytes, are the most common type of blood cell. During their lifetime, RBCs travel through blood vessels of various sizes, taking up oxygen in the lungs and releasing it into tissues while undergoing large passive deformations during repeated passage through the narrow capillaries of the microvasculature (Mohandas and Gallagher, 2008). Human RBCs take on average 20 seconds to complete one cycle of circulation. Survival of practically all other cells in the body depends upon the proper functioning of RBCs.

In humans, mature RBCs are non-nucleated cells, flexible and oval biconcave disks with a diameter of approximately 6.2–8.2 μm and a thickness at the thickest point of 2–2.5 μm and a minimum thickness in the center of 0.8–1 μm, being much smaller than most other human cells.

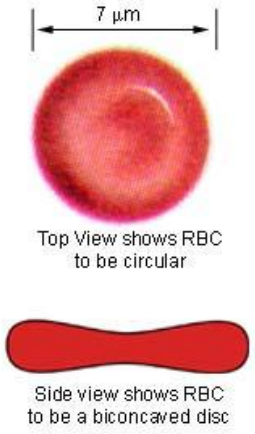

Figure 1. Schematic representation of red blood cell.

A normal RBC is a biconcave disk to achieve a maximum surface area to cytoplasmic volume ratio.

The cytoplasm of RBCs is rich in hemoglobin (Hb), an iron-containing biomolecule that can bind oxygen and is responsible for the red color of the cells.

The cell membrane is composed of proteins and lipids, and this structure provides properties essential for physiological cell function such as deformability and stability while traversing the circulatory system and specifically the capillary network.

Mature RBCs in mammals lack a cell nucleus and most organelles, in order to accommodate maximum space for Hb. The cells develop in the bone marrow and circulate for about 100–120 days in the body before their components are recycled by macrophages.

1.1. Life cycle of RBCs

Human RBCs are produced through a process named erythropoiesis, developing from stem cells to mature erythrocytes in about 7 days. Through this process RBCs are continuously produced in the red bone marrow of large bones and this production can be stimulated by the hormone erythropoietin (EPO), synthesized by the kidney. Normal adult humans produce and release into the circulation approximately 2×10^{11} new RBCs each day. The newly produced cells have extruded their nuclei in the bone marrow before they are released into the blood. However, these cells are irregularly shaped, have residual surface proteins of erythroblasts, and retain internal organelles including ribosomes, endoplasmic reticulum and mitochondria. Circulating reticulocytes are from 24 to 35% larger than the other erythrocytes in the blood so that during their 1–2 day maturation they lose about one-quarter of their volume and the residual internal organelles are degraded by multiple cellular processes including proteasomal degradation, autophagy, and vesicle exocytosis. Once a reticulocyte matures into a biconcave RBC, it will normally circulate for more than 110-120 days, but it will gradually lose about another 20% of its membrane and associated cytoplasm through exocytosis of vesicles that contain concentrated amounts of chemically modified Hb, including oxidized and glycated forms. (Koury, 2014)

At the end of their lifespan, they become senescent, and are removed from circulation. The aging RBCs undergoes changes in its plasma membrane, making it susceptible to selective recognition by macrophages and subsequent

phagocytosis in the mononuclear phagocyte system. This process is termed eryptosis and normally occurs at the same rate of production by erythropoiesis. (Lang and Qadri, 2012)

The spleen filters a portion of the RBCs through its red pulp, which contains capillary-like structures composed of macrophages that cull abnormally shaped or immunologically recognized RBCs from the filtered erythrocyte population before further transit through the red pulp space and reentry through slits in basement membranes of a large network of venous sinuses. (Koury, 2014)

Eryptosis is increased in a wide variety of diseases including sepsis, haemolytic uremic syndrome, malaria, sickle cell anemia, beta-thalassemia, glucose-6-phosphate dehydrogenase deficiency, phosphate depletion, iron deficiency and Wilson's disease. Eryptosis can be elicited by osmotic shock, oxidative stress, energy depletion as well as a wide variety of endogenous mediators and xenobiotics. (Lang and Qadri, 2012)

1.2. RBCs functions

RBCs cytosol consist mainly of hemoglobin (Hb), a complex metalloprotein containing heme groups whose iron atoms temporarily bind to oxygen molecules (O_2) in the lungs and release them throughout the body. Oxygen can easily diffuse through the RBCs plasma membrane. Hb in the RBCs also carries some of the waste product carbon dioxide back from the tissues; most waste carbon dioxide, however, is transported back to the pulmonary capillaries of the lungs as bicarbonate (HCO_3^-) dissolved in the blood plasma.

The blood plasma alone is straw-colored, but the red blood cells change color depending on the state of the Hb: when combined with oxygen the resulting oxyhemoglobin is scarlet, and when oxygen has been released the resulting deoxyhemoglobin is of a dark red color. Hb also has a very high affinity for carbon monoxide, forming carboxyhaemoglobin which is a very bright red in color.

1.2.1. Oxygen transport

Hb is an allosteric oxygen-transport protein. In adult humans the Hb molecule consists of four subunits, each having one polypeptide chain and one heme group. All Hbs carry the same prosthetic heme group iron protoporphyrin IX associated with a polypeptide chain of 141 (alpha) and 146 (beta) amino acid residues. The ferrous ion of the heme is linked to the N atom of a histidine. The porphyrin ring is wedged into its pocket by a phenylalanine of its polypeptide chain. The polypeptide chains of adult Hb themselves are of two kinds, known as alpha and beta chains, similar in length but differing in amino acid sequence. The alpha chain of all human Hb, embryonic and adult, is the same. The non-alpha chains include the beta chain of normal adult Hb ($\alpha_2\beta_2$). Oxygen binds reversibly to the ferrous iron atom in each heme group. The heme group that has become oxygen bound varies with the partial pressure of oxygen. The sigmoid shape of the oxygen equilibrium curve shows that there is cooperative interaction between oxygen binding sites. Hence, as oxygen action proceeds, combination with further molecules of oxygen is made easier. (Marengo-Rowe, 2006)

Hb function as an oxygen-carrier in the blood is fundamentally linked to the equilibrium between the two main states of its quaternary structure. Hb exists in two different conformational states, the T state being dominant in the absence of the ligand and the R state when the protein is fully saturated. The unliganded (deoxy) form is called the "T" (for "tense") state because it contains extra stabilizing interactions between the subunits. In the high-affinity R-state conformation the interactions which oppose oxygen binding and stabilize the tetramer are somewhat weaker or "relaxed". (Bellelli and Brunori, 2011)

Under the conditions of lower temperature, higher pH, and increased oxygen pressure in the capillaries of the lungs, the reaction proceeds to the right. The purple-red deoxygenated hemoglobin of the venous blood becomes the bright-red oxyhemoglobin of the arterial blood. Under the conditions of higher temperature, lower pH, and lower oxygen pressure in the tissues, the reverse reaction is promoted and oxyhemoglobin gives up its oxygen. (Bellelli and Brunori, 2011)

Although the oxygen transported by RBCs make possible cellular respiration throughout the body, RBCs lack mitochondria and so cannot perform cellular respiration themselves and must subsist on glycolysis.

1.2.2. Carbon dioxide transport

Carbon dioxide (CO_2) is generated in the tissues, but only about 5% of the CO_2 dissolves directly in the blood plasma. The 95% of the CO_2 coming from the tissues is carried in the RBCs. It enters and then leaves the cell by diffusion through the plasma membrane. Once inside, about one-half of the CO_2 is directly bound to Hb (at a different site from the one that binds oxygen).

The rest is converted by the enzyme carbonic anhydrase (CA) in carbonic acid, which dissociates into a hydrogen ion (H^+) and a bicarbonate ion:

$$\mathbf{CO_2 + H_2O \leftrightarrow H_2CO_3 \leftrightarrow H^+ + HCO_3^-}$$

Bicarbonate resulting from CA action, is transported into the plasma in exchange for extracellular chloride by band 3, the key protein for the blood's capacity to carry CO_2. When the RBCs reach the lungs, these reactions are reversed and CO_2 is released to the air of the alveoli. (Geers and Gros, 2000)

CAs are ubiquitous metalloenzymes participating in a variety of physiological and pathological processes that involve pH regulation, CO_2 and HCO_3^- transport, ion transport, biosynthetic reactions, bone resorption and tumorigenicity.

In mammals, 16 isozymes have been identified that differ in catalytic activity, subcellular localization and tissue distribution. RBCs typically express both (fast) CA II and higher concentrations of (slow) CA I. (Gilmour, 2010)

The biological functions of CAs are of great interest, as their contribution to the development of complications in some pathologies is not yet completely clarified. CA II plays an important role in the production of aqueous humour and much attention has been focused on the synthesis and characterization of CA II inhibitors, particularly in the treatment of glaucoma (Weiwei and Hu, 2009).

1.3. RBCs membrane: structure and function

The membrane of the RBCs plays many roles that aid in regulating their surface deformability, flexibility, adhesion to other cells and immune recognition. These functions are highly dependent on its composition, which defines its properties. The RBCs membrane is composed of 3 layers: the glycocalyx on the exterior, which is rich in carbohydrates; the lipid bilayer which contains many transmembrane proteins, besides its lipidic main constituents; and the membrane skeleton, a structural network of proteins located on the inner surface of the lipid bilayer. Half of the membrane mass in human RBCs are lipids and the other half are proteins. (Yazdanbakhsh et al., 2000)

1.3.1. Lipide domain

The main lipids are cholesterol and phospholipids. The RBCs membrane comprises a typical lipid bilayer, similar to what can be found in virtually all human cells. The lipid composition is important as it defines many physical properties such as membrane permeability and fluidity and also the activity of many membrane proteins is regulated by interactions with lipids in the bilayer.

Although cholesterol seems equally distributed between the two halves or leaflets of the lipid bilayer, the other lipids are asymmetrically distributed. Glycolipids, phosphatidylcholine and sphingomyelin are located in the outer half of the bilayer; phosphatidylinositols (PIs), phosphatidylethanolamine (PE) and phosphatidylserine (PS) occur in the interior layer facing the cytoplasm. (Smith, 1987)

This asymmetric phospholipid distribution among the bilayer is the result of the function of several energy-dependent and energy-independent phospholipid transport proteins. Proteins called “Flippases” move phospholipids from the outer to the inner monolayer, while others called “floppases” do the opposite operation, against a concentration gradient in an energy dependent manner. Additionally, there are also “scramblase” proteins that move phospholipids in both directions at the same time, down their concentration gradients in an energy independent manner. (Mohandas and Gallagher, 2008)

The maintenance of an asymmetric phospholipid distribution in the bilayer (such as an exclusive localization of PS and PIs in the inner monolayer) is critical for the cell integrity and function due to several reasons. Macrophages recognize and phagocytose RBCs that expose PS at their outer surface. Thus the confinement of PS in the inner monolayer is essential if the cell is to survive its frequent encounters with macrophages, especially in the spleen. (Mohandas and Gallagher, 2008)

An exposure of PS can potentiate adhesion of RBCs to vascular endothelial cells, effectively preventing normal transit through the microvasculature. Thus it is important that PS is maintained only in the inner leaflet of the bilayer to ensure normal blood flow in microcirculation. Both PS and phosphatidylinositol-4,5-bisphosphate (PIP2) can regulate membrane mechanical function, due to their interactions with proteins such as spectrin and protein 4.1R, modulating the linkage of the bilayer to the membrane skeleton.

Proteins in the lipid domain usually extend from the inside of the erythrocyte to the outside. These membrane proteins can be divided structurally into an internal hydrophilic portion, a membrane hydrophobic portion, and an external hydrophilic portion with attached carbohydrates. (Smith, 1987)

Integral proteins include several glycophorins, aquaporins and protein band 3.

The **glycophorins** (2% of RBC membrane proteins) are glycosylated in their extracellular domain and imparts a negative charge to the cell, reducing interaction with other cells/ endothelium.

The **aquaporins** are selective pores for water transport and allow RBCs to remain in osmotic equilibrium with extracellular fluid.

The membrane protein **band 3** serves simultaneously as an anion exchanger (plays a critical role in the CO_2 transport system), an anchor for the cytoskeleton, Hb and glycolytic enzymes and as a senescence antigen.

1.3.2. Cytoskeleton

Membrane-associated cytoskeletal protein networks are involved in the control of cell shape, attachments to other cells and to the substrate, and in organization of

specialized membrane domains. Cytoskeletal proteins interact with integral proteins and lipids of the bilayer to maintain membrane integrity.

The cytoskeleton of RBCs form a filamentous network under the lipid bilayer and consists of several proteins such as spectrin, ankyrin, actin, and protein 4.1.

Spectrin is the most prominent component of the RBCs membrane cytoskeleton. It is a fibrous polypeptide constituted by two isoforms, alpha (260 kDa) and beta (225 kDa). Both proteins are long, flexible structures that are twisted together to form heterodimers (Smith, 1987). Tetramers, and possibly higher order oligomers, are formed by a "head-to-head" interaction of heterodimers. Two alpha-beta helixes are linked end to end to form a single tetramer, which has binding sites for several other proteins, including other spectrin molecules. The spectrin tetramers are organized into a meshwork that is fixed to the membrane by the protein ankyrin. Actin binds to the "tail" of several heterodimers to generate a series of polygons (mostly hexagons), with spectrin tetramers as the sides. (Luna and Hitt, 1992)

Ankyrin is itself connected to a transmembrane protein band 3. The purpose of band 4.2 (palladin, 72 kDa) may be to stabilize the link between ankyrin and the anion exchanger. Spectrin is also linked to a transmembrane protein called glycophorin C (25 kDa) by the protein known as band 4.1. Thus the meshwork is anchored to the membrane at multiple sites. (Luna and Hitt, 1992)

Actin subunits (subunit mass of 43 kDa), actually form short microfilaments consisting of filamentous actin and tropomyosin (isoforms of 27 and 29 kD). The protein tropomodulin is also associated with filamentous actin. Band 4.9 protein, known also as dematin (48 kDa) may crosslink some of the actin microfilaments to make bundles of f (filamentous) actin.

Membrane protein **Band 4.1** (78 kDa) promotes and stabilizes the association of spectrin with actin as does the protein adducin. (Luna and Hitt, 1992)

1.4. Protein Band 3

Band 3 is a multifunctional transmembrane protein, which is the most abundant protein in the RBCs plasma membrane ($1.2\times l0^6$ copies per cell, about of 25% of

the total membrane protein) (Low, 1986). The protein band 3 is an anion exchanger (Anion Exchanger 1- AE1, SLC4A1), expressed in erythroid cells and the kidney, but also serves as a protein anchor, connecting soluble cytoplasmic proteins and components of the cytoskeleton to the membrane, hemoglobin, and glycolitic enzymes, as well as a senescence antigen (Tanner, 2002)

This integral protein (911 amino acid; 95 kDa) has three distinct functional domains: the large N-terminal domain and short C-terminal tail of the protein are both located in the cytoplasm and the transmembrane domain (Fig. 2).

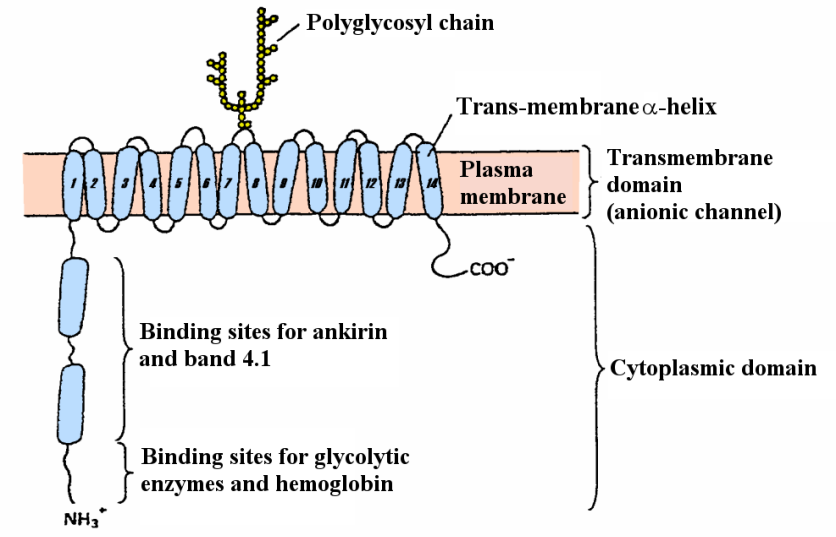

Figure 2. Structural domains of RBCs protein band 3.

The N-terminal domain (Cdb3) (residue l-360; molecular weight of 43 kDa) not only anchors the RBCs skeleton by association with ankyrin and protein 4.1 but also binds an array of other proteins, including protein 4.2, the glycolytic enzymes glyceraldehyde 3-phosphate dehydrogenase, aldolase and phosphofructokinase the tyrosine kinase p72syk and deoxyhemoglobin.

The C-terminal domain (amino acids 361–911; 52 kDa) comprises 12–14 transmembrane (TM) segments with a short (33 amino acid) cytoplasmic tail. The C-terminal tail harbors a binding site for carbonic anhydrase II (CA II), essential for the erythrocyte-based system that moves carbon dioxide from the tissues to the lungs. The central integral membrane domain performs chloride-bicarbonate

exchange, also contains a single N-linked glycosylation site on its extracellular surface that is not required for transport. (Van den Akker et al., 2010)

The main functions of band 3 may be summed up into: **anion exchanger**, **anchor of proteins** and **marker of senescence**.

Band 3 multi-spanning integral membrane domain has an **anion exchanger** function and plays a critical role in the CO_2 transport system. Since the solubility of carbon dioxide in the blood is rather low, the CO_2 molecule which diffuses into the RBCs through the plasma membrane is converted into HCO_3^- by cytosolic carbonic anhydrase. The bicarbonate anion is then transported out of the cell by the band 3 protein in exchange for a Cl^- anion. When the blood reaches the lung, the above exchange process is reversed as a result of a CO_2 pressure gradient between the blood and the lung alveoli. One site of band 3 expression is in the kidney where its anion exchange activity may have a role in pH regulation of blood. (Jennings, 1985; Wang, 1994; Jay, 1996)

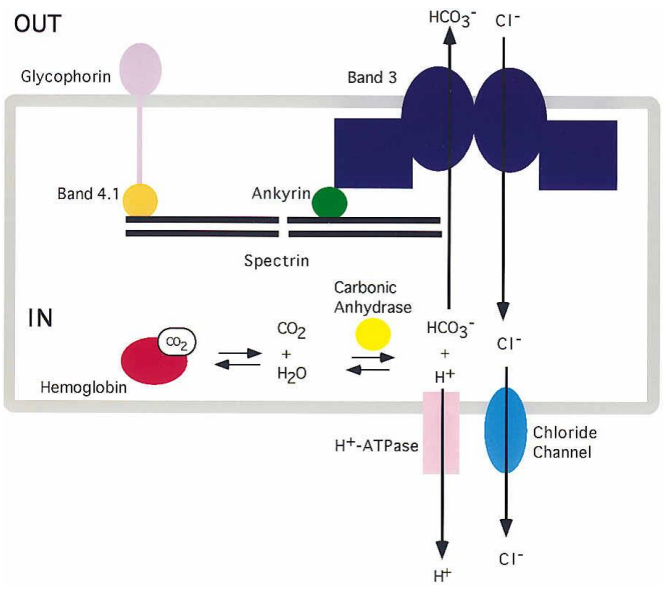

Figure 3. The interactions of band 3 in cell shape, anion exchange, and pH regulation. (Jay, 1996)

Band 3, also serves as a **protein anchor**, connecting soluble cytoplasmic proteins and components of the cytoskeleton to the membrane. Spectrin binds to band 3 via

ankyrin and band 4.1 (Fig. 3). These interactions with cytoskeletal proteins make band 3 essential for maintaining cell shape and mechanical strength.

It is also known that this protein guarantees glycolysis regulation through protein/enzymes binding to its cytoplasmic tail (Ferru et al., 2011) and provides binding sites for Hb, hemichrome (Fig. 4). (Wang, 1994; Pantaleo et al., 2008)

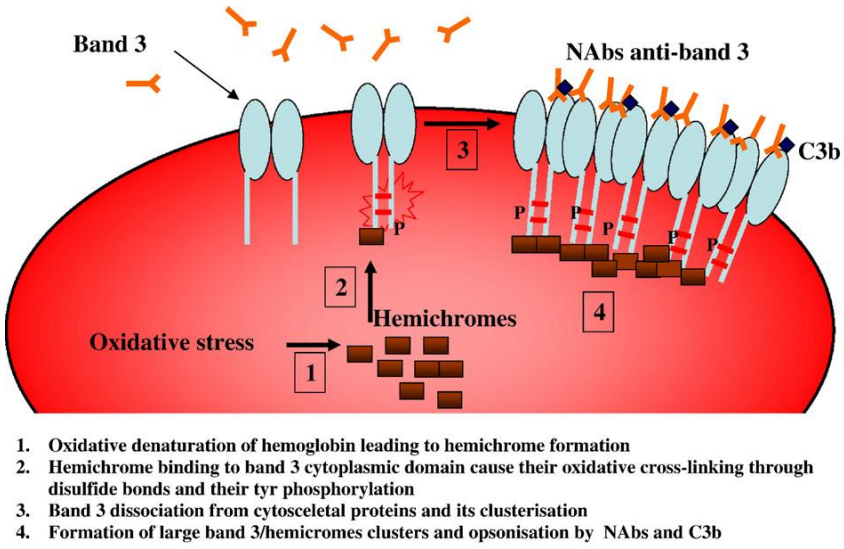

Figure 4. (Pantaleo et al., 2008)

Band 3 also has a third function. The external RBCs surface is non-immunogenic and non-adhesive, to avoid adhesion to endothelia and phagocytosis by spleen, liver and bone marrow macrophages, ready to eliminate any cell showing even subtle membrane alterations. Internally, the continuous formation of oxidant species during the oxygenation-deoxygenation cycles of Hb are opposed by powerful detoxication and protection mechanisms of RBCs. What determines the RBCs demise is not its fragmentation but its rapid transformation into a non-self cell, recognized as such by the phagocytic system and removed. This transformation is likely due to rather subtle modifications of the RBCs membrane and expression of neo-antigenic sites that lead to opsonization or direct recognition by phagocytes. The protein band 3 acts as a **senescence antigen** for aged and damaged red cells. Clustering of band 3 in the RBCs membrane triggers binding of antibodies to an extracellular part of the protein (Fig. 4) and causes the removal of aged or damaged red cells. (Pantaleo et al., 2008; Arese et al., 2005)

1.4.1. Band 3 and membrane proteins interaction

The membrane integral proteins establish linkages with cytoskeletal proteins and may play an important role in regulating cohesion between the lipid bilayer and cytoskeleton, likely enabling the RBCs to maintain its favorable membrane surface area by preventing the membrane from collapsing (vesiculating).

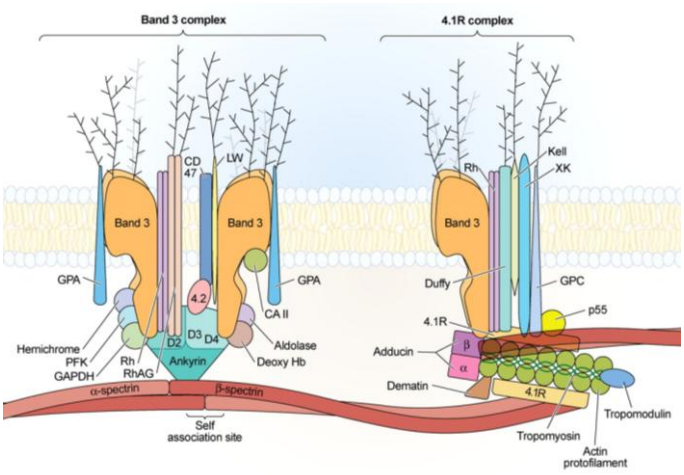

Figure 5: Schematic representation of two types of multiprotein complexes in the red cell membrane. (Salomao et al., 2008)

Protein complex (Left side of Fig. 5) attached to spectrin near the center of the tetramer (dimer–dimer interaction site). Tetrameric band 3 is bound to ankyrin, which is bound to spectrin. The membrane skeletal protein 4.2 has binding sites for band 3 and for ankyrin. Transmembrane glycoproteins GPA, Rh, and RhAG bind to band 3, and CD47 and LW associate with Rh/RhAG. The two cytoplasmic domains of band 3 contain binding sites for soluble proteins, the short C-terminal domain for cytosolic carbonic anhydrase II (CA II), the large N-terminal domain for deoxyhemoglobin and for glycolytic enzymes, aldolase, phosphofructokinase (PFK), and glyceraldehyde 3′-phosphate dehydrogenase (GAPDH).

The right side of the Fig. 5 shows protein complex at membrane cytoskeletal junctions. The junctions contain the ternary complex of spectrin, F-actin, and 4.1R, as well as the actin-binding proteins tropomyosin, tropomodulin, adducin, and dematin. 4.1R enters into an additional ternary interaction with the

transmembrane protein GPC and p55 and is taken also to bind to band 3, in the form of a dimer, which also carries GPA. (Salomao et al., 2008).

1.4.2. Band 3 tyrosine-phosphorylation

Phosphorylation/dephosphorylation of protein tyrosine residues (Tyr) has been implicated in the regulation of several RBCs functions, including metabolic pathways (Harrison et al., 1991; Low et al., 1993; De Neef et al., 1996) membrane transport (De Franceschi et al., 1997; Musch et al., 1999) and cellular volume and shape (Musch et al., 1999; Bordin et al., 1995; Minetti et al., 1998).

Protein tyrosine kinases (PTKs) identified to date in RBCs include insulin receptor tyrosine kinase (Herzberg et al., 1980) and the Syk (Harrison et al., 1994; Brunati et al., 1996) and Src-like non-receptor tyrosine kinases (Brunati et al., 1996; De Franceschi et al., 1997). Among the Src-like tyrosine kinases detected in human RBCs, Lyn and Fgr are expressed predominantly, with Hck being found at a lower levels (De Franceschi et al., 1997). The attempt at purifying the native protein tyrosine kinases from RBCs led to the isolation of substantial amounts of only the 2 tyrosine kinases, Syk and Lyn. (Brunati et al., 1996)

The PTKs belonging to the Src family share a high degree of structural similarity, with a common domain architecture and regulatory mechanisms. The Src sequence consists of a poorly conserved N-terminal segment, 2 conserved domains termed Src homology 3 (SH3) and SH2, followed by the catalytic domain, SH1 (Brown and Cooper, 1996). The SH3 and SH2 domains interact with protein sequences containing polyproline II helices and phospho-Tyr residues, respectively, and play a dual role in Src regulation, because they are both required for keeping Src kinase in an inactive state and targeting the enzyme to specific substrates (Xu et al., 1997).

The activity of Src-related kinases is modulated by phosphorylation of 2 tyrosine residues: autophosphorylation of Tyr 416 (c-Src numbering), located inside the catalytic domain, correlates with enzyme activation,14,18-20 while Csk-mediated phosphorylation of the C-terminal Tyr 527 gives rise to inactive forms of Src kinases. Indeed, phosphorylated Tyr 527 interacts with the SH2 domain of the Src

molecule, thus triggering a reorganization of the enzyme structure that forces the kinase to adopt a locked and down-regulated conformation (Xu et al., 1997).

Syk (p72syk) which is comprised of two tandemly arranged SH2 domains, a linker region that is postulated to bind cellular effectors, a catalytic domain that includes autophosphorylation sites, and a short carboxyl-terminal extension.

SHP-2 is a non-transmembrane **protein tyrosine phosphatases** (PTPs) involved in the signaling pathway of a variety of growth factors and cytokines and plays an important role in relaying signals from the cell surface to the nucleus. It is expressed in human RBCs, where it is mostly present in the cytosol. SHP-2 containing 2 SH2 domains and interacts with many proteins by recognizing specific Tyr-phosphorylated motifs through its amino-terminal SH2 domain (Donella-Deana et al., 1998). This protein–protein interaction enhances SHP-2 activity by relieving the inhibitory intramolecular interactions between the amino-terminal SH2 domain and the catalytic phosphatase domain. Thus, the SH2 domains play a crucial role both in the recruitment of cellular substrates and in the modulation of the enzyme catalytic activity (Brunati et al., 2000).

The Tyr-phosphorylated state of cellular proteins reflects the balance between the competing activities of PTKs and PTPs. Because the activity of PTPs is much higher than that of PTKs, basal levels of protein Tyr-phosphorylation (Tyr-P) in cells are very low (Brautigan, 1992; Walton and Dixon, 1993).

Treatment of human RBCs with pervanadate, diamide, or N-ethylmaleimide (NEM), which act as both oxidizing agents and PTPs inhibitors, induces an increase in protein Tyr-P. Under these conditions, the multifunctional transmembrane band 3 has been demonstrated to represent the main Tyr-phosphorylated protein (Harrison et al., 1994; Brunati et al., 2000).

Band 3 has four Tyr-phosphorylatable sites (Fig. 6): Tyr 8, located in the highly acidic cytoplasmic domain, has been identified as the major Tyr-P site in vitro; Tyr 21, Tyr 359 and Tyr 904 have also been reported to be phosphorylated in vitro. (Yannoukakos et al., 1991).

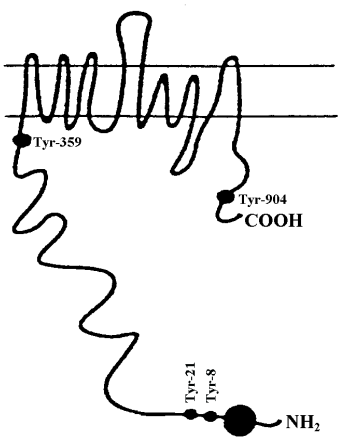

Figure 6. Schematic representation of band 3 Tyr-phosphorylatable sites.

Two well characterized protein kinases, Syk (p72syk) and Lyn (p53/56lyn), are thought to be responsible for the vast majority of band 3 tyrosine phosphorylation (Harrison et al., 1994). Protein tyrosine kinase Syk catalyzes the so-called "primary phosphorylation" of band 3 at Tyr 8 and 21 within the cytoplasmic domain of the polypeptide (Fig. 7). (Bordin et al., 2005a)

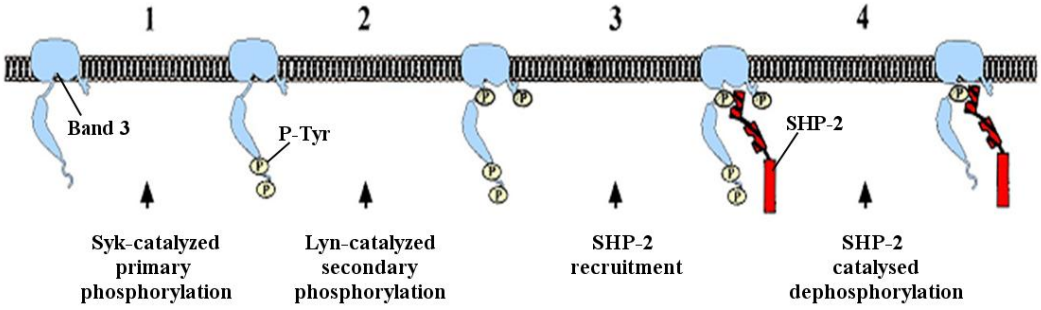

Figure 7. Sequential steps underlying the mechanism of phosphorylation and dephosphorylation of protein tyrosine residues (Tyr) of band 3 in treated human RBCs.

Subsequently, Lyn, recruited to band 3 through an interaction between its SH2 domain and one of the above mentioned phospho-Tyr, catalyzes the "secondary phosphorylation" of band 3 at Tyr 359 and 904 (Brunati et al., 2000). The localization of Lyn next to its phosphorylation sites can be easily explained by its binding to phosphorylated tyrosines 8 and 21 of band 3, which are positioned in the crystal structure adjacent to both Tyr359 and the membrane-spanning domain

of band 3.SHP-2, located in the RBCs cytosol, is recruited to the membrane when there is increased of band 3 Tyr-P. Band 3 is both anchoring protein and substrate for the SHP-2 (Bordin et al., 2002). Upon binding of the N-terminal SH2 domain to a specific P-Y359 target, the enzyme adopts an “open” active conformation and catalyzes band 3 dephosphorylation on residues Tyr 8, Tyr 21, and Tyr 904 (Bordin et al., 2002).

1.5. RBCs and oxidative stress

Reactive oxygen species (ROS) are chemically reactive molecules containing oxygen. ROS form as a natural product of the normal metabolism of oxygen and have important roles in cell signalling and homeostasis. Effects of ROS on cell metabolism include roles in apoptosis, positive effects such as the induction of host defence genes and mobilisation of ion transport systems.

Normally, cells defend themselves against ROS damage with enzymes such as superoxide dismutases, catalases, lactoperoxidases, glutathione peroxidases and peroxiredoxins. Small molecule antioxidants such as ascorbic acid (vitamin C), tocopherol (vitamin E), uric acid and glutathione also play important roles as cellular antioxidants. In similar manner, polyphenol antioxidants assist in preventing ROS damage by scavenging free radicals.

Oxidative stress (OS) reflects an imbalance between the generation of ROS and a biological system's ability to readily detoxify the reactive intermediates or to repair the resulting damage. Chemically, OS is associated with increased production of oxidizing species or a significant decrease in the effectiveness of antioxidant defences. In general, harmful effects of ROS on the cell are most often: damage of DNA, lipid peroxidation, oxidations of amino acids in proteins, inactivation of specific enzymes by oxidation of co-factors and disruptions in normal mechanisms of cellular signalling.

RBCs are cells circulating in direct contact with plasma containing steroids, proteins or inflammation-related products, such as ROS.

Many proteins are susceptible to attack by ROS, especially on sulfhydryl groups which are among the most easily oxidized protein residues. Oxidation can lead to

inter- and/or intra-molecular cross linking thus inducing protein degradation (Stadtman and Levine, 2000; Pacifici and Davies, 1990), clustering (Bordin et al., 2010a) and enzyme inactivation (Bordin et al., 2010a; Bordin et al., 2005b).

S-Glutathionylation is the post-translational modification of protein cysteine residues by the addition of glutathione, the most abundant and important low-molecular-mass thiol within most cell types. This post-translational process occurs through the reversible addition of a proximal donor of glutathione to thiolate anions of cysteines in target proteins, where the modification alters molecular mass, charge, and structure/function and/or prevents degradation from sulfhydryl overoxidation or proteolysis. For translational application, S-glutathionylated proteins may be useful as biomarkers in individuals exposed to agents that cause oxidative or nitrosative stress. (Grek et al., 2013)

When treated with diamide, a mild oxidant which induces cysteine disulfide bond formation and inhibits tyrosine (Tyr)-protein phosphatase activities (Bordin et al., 2005a; Bordin et al., 2006), RBCs show a well-defined Tyr-P level of membrane proteins, particularly of band 3 (Bordin et al., 2006). This protein has long been involved in the senescent process of human RBCs (Lutz et al., 1988; Bosman et al., 2005), through mechanisms of either proteolytic fragmentation (Bosman et al., 2010) or clustering (Bordin et al., 2010a; Bosman et al., 2005), both triggering IgG recognition and binding (Bordin et al., 2010a; Lutz et al., 1988). This, in turn, allows further recognition and phagocytosis by macrophages which eliminate senescent/altered RBCs. (Lutz et al., 1988; Bosman et al., 2005; Bosman et al., 2010; Bratosin et al., 1998)

Alterations in diamide-induced band 3 Tyr-P levels represent pre-existing membrane status modifications, like those observed in glucose-6-phosphate dehydrogenase (G6PD)-deficient patients (Bordin et al., 2010a; Bordin et al., 2005b), suffering chronic impairment of antioxidant defenses, or in patients with endometriosis (Bordin et al., 2010b) or polycystic ovary syndrome (PCOs) (Donà et al., 2012), with systemic inflammation. Diamide triggers band 3 Tyr-P (Bordin et al., 2005a; Bordin et al., 2005b; Bordin et al., 2006) and aggregation in high

molecular weight aggregates (HMWA), both useful parameters in the evaluation of oxidation-related damage to cells (Bordin et al., 2010a; Bordin et al., 2006).

2. ALDOSTERONE

Aldosterone (Aldo) is a steroid hormone (mineralocorticoid family) produced by the outer section of the cortex (zona glomerulosa) in the adrenal gland.
As the name of this class of hormones implies, the mineralocorticoids control the excretion of electrolytes.

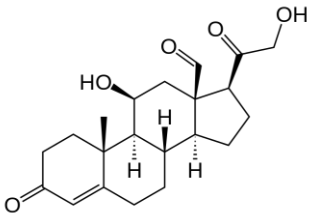

Figure 8. Molecular structure of aldosterone.

Aldo plays a central role in the regulation of blood pressure mainly by acting on the distal tubules and collecting ducts of the nephron, increasing reabsorption of sodium and water in the kidney, potassium secretion and sustains a constant extra cellular fluid volume (Funder, 2010). However, the action of Aldo is exerted on sweat glands, stomach, and salivary glands to the same effect, i.e. sodium reabsorption. This action is accompanied by the retention of chloride and water resulting in the expansion of extracellular volume.

2.1. Aldosterone synthesis and regulation

The corticosteroids are synthesized from cholesterol within the zona glomerulosa of adrenal cortex. Many of the enzymes of adrenal steroid hormone synthesis are of the class called cytochrome P450 (CYP).
Aldosterone and corticosterone share the first part of their biosynthetic pathways.

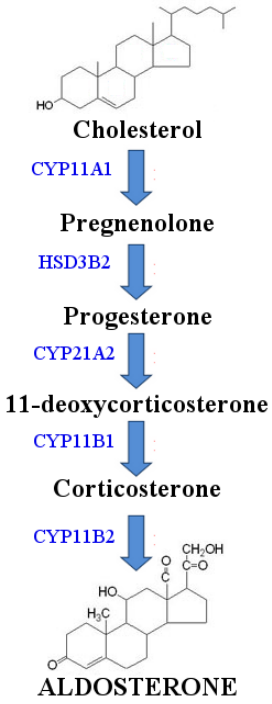

Figure 9. Aldosterone biosynthesis from cholesterol.

In order for cholesterol to be converted to pregnenolone in the adrenal cortex it must be transported into the mitochondria where CYP11A1 resides. This transport process is mediated by steroidogenic acute regulatory protein (StAR) and it is the rate-limiting step in steroidogenesis.

Conversion of pregnenolone to progesterone requires the enzyme 3β-hydroxysteroid-dehydrogenase type 1 (gene symbol HSD3B2) and the enzyme 11β-hydroxylase (CYP11B1) transforms 11-deoxycorticosterone in corticosterone.

Zona glomerulosa cells are unique in the adrenal cortex in containing the enzyme responsible for converting corticosterone to aldosterone, the principal and most potent mineralocorticoid. This enzyme is CYP11B2, also called aldosterone synthase. (Connell and Davies, 2005)

2.1.1. The role of the renin-angiotensin system

Renin is synthesized and released by the juxtaglomerular cells in the afferent arteriole of the kidney in response to a decrease in intravascular volume detected

by baroreceptors. Pressure-sensitive baroreceptors are found in the vessel walls of nearly all large arteries in the thorax and neck, in particular in carotid arteries and in the aorta. These specialized receptors are sensitive to changes in mean arterial pressure and detect low blood pressure or low blood volume. In response to hypotension, renin is released by the kidney and cleaves angiotensinogen into angiotensin I, which is converted to angiotensin II by angiotensin converting enzyme (ACE). Angiotensin II acts on vascular smooth muscle to cause vasoconstriction, and on the adrenal zona glomerulosa to stimulate aldosterone production. The adrenal response to Ang II occurs within minutes, a time course that implies that no new protein synthesis is required (Connell and Davies, 2005).
Angiotensin II and a variety of secondary factors (potassium and sodium concentrations, adrenocorticotropic hormone (ACTH) and vasopressin) induce Aldo synthesis in adrenal zona glomerulosa cells. Aldo is released to the circulation, promotes sodium retention in the kidney, and exerts direct effects in the heart and other organs (Spat and Hunyady, 2004).

2.1.2. Other regulator factors

Aldo has an essential role in maintaining extracellular fluid and thereby circulation and its secretion is controlled by several factors. Most or all increases in Aldo secretion may be attributable to increased activity of the renin-angiotensin system and/or increased plasma level of K^+.
Under physiological conditions the control of secretion is probably confined to the stimulatory factors ACTH, angiotensin II (ANG II), and K+ concentration.
Aldo secretion is also increased during acute or chronic sodium depletion, fluid or blood loss, erect postural position, dietary potassium loading, tissue damage leading to hyperkalemia and pregnancy.
When sodium or fluid loss is severe, ACTH is also secreted and synergizes with ANG II or K^+ in stimulating glomerulosa cells. Inhibitory factor atrial natriuretic hormone (ANP) secretion is increased in response to sodium and/or water loading, and it in turn inhibits aldosterone secretion. (Hattangady et al., 2012)

The aldosterone production is also affected to one extent or another by nervous control, which integrates the inverse of carotid artery pressure, pain, posture and probably emotion.

2.2. Aldosterone functions

The steroid hormone Aldo controls sodium and potassium balance and also influences acid-base homeostasis of the vertebrate organism.

Its major physiological targets are the epithelial cells, of which the most important are located in the distal nephron. Aldo augments Na^+ reabsorption as well as K^+ and H^+ excretion, acting on the nuclear mineralocorticoid receptors (MR) within the cells of the distal tubule and the collecting duct of the kidney nephron. In these cells Aldo upregulates and activates the basolateral Na^+/K^+ pumps and this in turn results in reabsorption of sodium (Na+) ions and water (which follows sodium) into the blood and secretion of potassium (K+) ions into the urine (Briet and Schiffrin, 2011).

Aldo upregulates also epithelial sodium channels (ENaCs), increasing apical membrane permeability for Na^+. Cl^- is reabsorbed in conjunction with sodium cations to maintain the system's electrochemical balance. Through changes in sodium balance, Aldo influences the extracellular fluids and blood pressure.

In addition to its epithelial actions, Aldo influences the function of various non-epithelial tissues, particularly the cardiovascular system and central nervous system (CNS). In contrast to its established effects on electrolyte balance in epithelial tissue, Aldo in the cardiovascular system promotes cardiac hypertrophy, fibrosis and abnormal vascular endothelial function. In the CNS, it appears to regulate blood pressure, salt appetite and sympathetic tone. (Connell and Davies, 2005).

2.3. Genomic and non-genomic pathway

Aldo exerts its function by binding to classical mineralocorticoid receptor (MR) acting as ligand-dependent transcription factor (Robert-Nicoud et al., 2001; Yang and Fuller, 2012). Over the last decade, there has been an increasing amount of evidence showing the dual effect of Aldo. In the first pathway, termed "genomic", Aldo binds to the MR which, being linked to several other proteins in a cytosolic complex, dissociates and translocates to the nucleus to regulate target gene expression (Yang et al., 2011).

The MR is expressed in renal epithelial cells and also in non-epithelial tissue such as the heart and the brain. Aldosterone exerts its effects on water homeostasis by transcriptional regulation of serum-glucocorticoid regulated kinase 1 (Sgk1), epithelial sodium channels (ENaC), sodium-potassium-ATPase, and other entities in renal collecting duct cells. (Lother et al., 2014)

In the second pathway, Aldo elicits rapid "non-genomic" effects on second messenger systems and signaling cascades of different tissues (Boldyreff and Wehling, 2003; Dooley et al., 2012). Aldo mediates rapid effects such as the activation of protein kinase C (PKC), protein kinase D (PKD), extracellular signal-regulated kinase (ERK1/2) and mitogen-activated protein kinase (MAPK) cascades through the transactivation of the epidermal growth factor receptor (EGFR), via the non-receptor tyrosine kinase, c-Src. Signalling cascades coupled to EGFR transactivation either directly modulate membrane targets through their phosphorylation or alternatively modulate the expression of membrane targets through the phosphorylation of transcription factors such as CREB or MR. (Dooley et al., 2012)

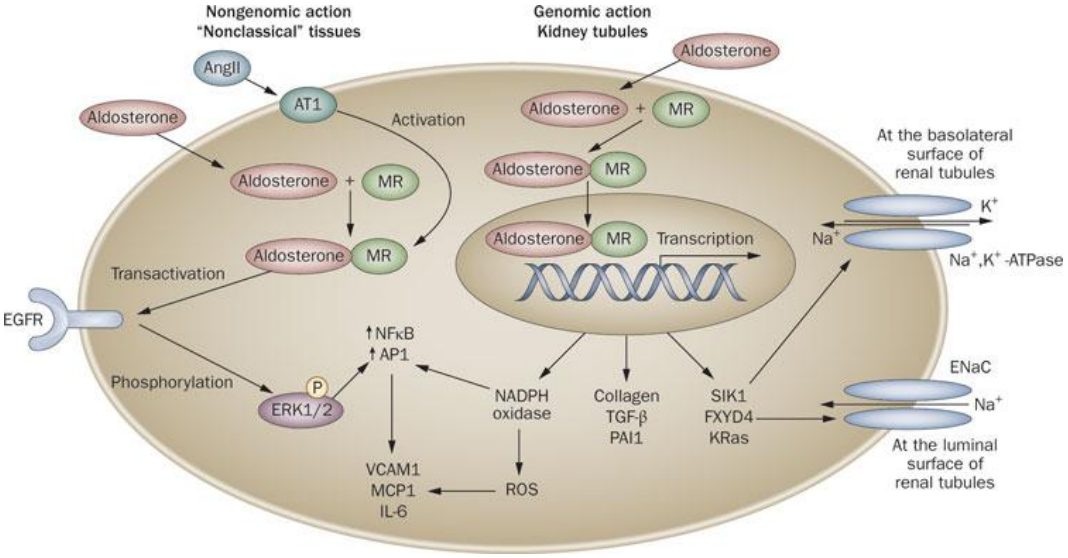

Figure 10. Genomic and nongenomic actions of aldosterone and interaction with the mineralocorticoid receptor. (Lastra et al., 2010)

Inappropriately high plasma level of Aldo contribute to progressive organ damage to the heart (Reil et al., 2012; Funder, 2010; Funder, 2011), vasculature (Rocha et al., 1998) and kidney (Shibata and Fujita, 2012; Egido, 1996; Berl et al., 1978), promoting myocardial (Swynghedauw, 1999; Qin et al., 2003; Nakamura et al., 2009) and vascular fibrosis (Tylicki et al., 2008), oxidative stress (Patni et al., 2007; Pu et al., 2003) and perivascular inflammation (Pu et al., 2003).

2.4. Aldosterone and oxidative stress

The hypothesis of Aldo induced oxidative stress was confirmed in patients with chronic heart failure since they showed increased amounts of plasma markers of oxidative stress, e.g. oxidized low-density lipoprotein and 8-isoprostane (Kotlyar et al., 2006; Yamaji et al., 2009). Macrophages isolated from these patients, after treatment with the MR blocker spironolactone, exhibited lower levels of superoxide release and lipid peroxides than macrophages taken before the spironolactone treatment (Keidar et al., 2005), revealing an important systemic source of MR-induced oxidative stress. Also, in patients with essential hypertension, who often present criteria of hyperaldosteronism, plasma markers of

oxidative stress (OS) like isoprostanes were elevated (Laffer et al., 2006; Stehr et al., 2010).

A first investigation of Aldo-mediated effects on human cells was conducted on cells isolated from an adrenal adenoma in comparison to cells from normal adrenal tissue. In the adenoma cells, which had been exposed to high concentrations of the locally produced Aldo, the expressions of anti-oxidative proteins as well as the expression of the superoxide generating enzyme NADPH oxidase were increased (Calò et al., 2010).

3. MINERALOCORTICOID RECEPTOR

The mineralocorticoid receptor (MR) derived from the NR3C2 gene, belongs to the steroid/thyroid hormone receptor super-family including glucocorticoid (GR), thyroid (THRA, THRB), retinoic acid (RAR), vitamin D (VDR) and other orphan receptors. In humans, the NR3C2 gene located in the locus 4q31.1, encodes for a 984 amino acids (aa) protein that makes MR the largest steroid receptor (Faresse, 2014). As all the nuclear receptors, the MR protein structure is divided in three domains; a N-terminal domain (NTD) of 602 aa involved in the control of the transcriptional activity of the receptor; the central DNA-binding domain (DBD) of 66 aa involved in the binding of the specific response element found on the promoter of MR target genes; and finally a ligand-binding domain (LBD) of 251 aa responsible for the selectivity of hormone binding (Faresse, 2014). The high homology of MR LBD with GR LBD, allows MR to bind two types of hormones: the mineralocorticoids, represented principally by aldosterone, and the glucocorticoids represented by and cortisol in humans (Baker et al., 2013).

Upon hormonal activation, MR is translocated into the nucleus, where it binds to transcriptional co-factors to regulate the expression of target genes. The nuclear translocation of MR can be achieved either as a homodimer, or associated to GR as a heterodimer.

The ligand-dependent transcription, also called the late response (after 30 min to 1h), is well characterized and induces the regulation of hundreds of target genes.

These genes present a palindromic DNA sequence common for GR and MR called glucocorticoid response element within their promoter (Fuller et al., 2000).
A unique response element specific for MR has not been yet identified. In addition to the late response, an early response has been also described. This early phase occurs within minutes after ligand treatment and activates a variety of second messengers (Grossmann and Gekle, 2009).
The MR-positive tissues can be divided in two groups: the epithelial and non-epithelial tissues. Given the high concentration of circulating glucocorticoids (100–1000 fold higher than Aldo) it was proposed that glucocorticoids are the principal ligand of MR in these tissues (Connell and Davies, 2005).
However, in epithelial tissues, such as nephron, colon, trachea or salivary glands, MR expression is always associated with the 11-β-hydroxysteroid dehydrogenase 2 (11-β-HSD2) that allows the selectivity of MR binding to Aldo by converting the glucocorticoids to their inactive forms (Albiston et al., 1994; Baker et al., 2013).
The regulation of MR signaling can occur at different levels: the amount of hormone available locally, the interacting proteins in the cytoplasm and in the nucleus as transcriptional co-factors, the regulation of the nucleo-cytoplasmic shuttling, the cross-talk with other signaling pathways and finally the post-translational modifications (PTMs) of the receptor. Numerous modifications have been characterized including phosphorylation, glycosylation, ubiquitylation, neddylation, nitrosylation, methylation, acetylation, sumoylation and lipidation. These PTMs are able to regulate all aspects of normal cell biology and pathogenesis (Faresse 2014).

4. PRIMARY ALDOSTERONISM

Primary Aldosteronism (PA) is the most common form of endocrine hypertension characterized by excessive Aldo secretion by the adrenal glands, relatively autonomous of the renin-angiotensin system (RAS).

This overproduction of Aldo is not a consequence of excessive renin stimulation but results from autonomous secretion from the adrenal cortex. It is caused in the majority of cases by a unilateral aldosterone producing adenoma or bilateral adrenal hyperplasia and is often accompanied by hypokalemia (Zennaro et al., 2014).

Only a minority of the PA cases are familial and due to known (CYP11B2/CYP11B1 chimeric gene or mutations in the KCNJ5 gene) or unknown causes (Lenzini and Rossi, 2014).

Although Aldo excess is directly linked to the development of hypertension through renal sodium and water retention it also induces tissue inflammation with subsequent fibrosis and remodeling in organs such as the kidney (Shibata and Fujita, 2012; Egidio, 1996), heart and vasculature (Reil et al., 2012; Funder, 2010; Rocha et al., 1998). As a consequence, PA leads to the development of renal impairment, atrial fibrillation (Reil et al., 2012), stroke and myocardial infarction (Funder, 2010; Rocha et al., 1998).

However, due to the absence of PA related specific symptoms and signs there is substantial delay in establishing the diagnosis that may affect the response to treatment and overall prognosis. Thus, early diagnosis is of paramount importance in order to initiate specific treatment by either surgical removal of the hyperfunctioning adrenal lesion(s) or administration of targeted medical treatment with mineralocorticoid receptor antagonists (Zennaro et al., 2014).

AIM OF THE STUDY

In previous studies (Bordin et al., 2005b; Donà et al., 2012; Bordin et al., 2010b; Andrisani et al., 2014), we identified in the Tyr-P process of RBC membrane band 3 an important parameter able to discriminate between normal volunteers and patients with inflammatory diseases, such as glucose 6 phosphate dehydrogenase deficiency (G6PDd), polycystic ovary syndrome (PCOs) and endometriosis. In all these pathologies the common feature was an impairment of the GSH-related antioxidant activities, situation leading to RBCs membrane alterations. In un-treated conditions, no difference between healthy controls and patients may be seen, but, in the presence of diamide, blind oxidant, enhanced Tyr-P levels in patients are clearly found. More interestingly, the increases of Tyr-P in membranes are directly proportional to the extent of the oxidizing-related parameters, such as lowering of the cytosolic glutathione following diamide treatment and increase in glutathionylated membrane proteins.

Aldosterone (Aldo), besides regulating fluid and electrolyte homeostasis by stimulating gene expression of proteins involved in Na+ and K+ regulation and reabsorption in renal tissues, can also induce oxidative stress (Patni et al., 2007) and perivascular inflammation (Pu et al., 2003) by directly activating or inducing gene expression of NADPH oxidase system. For this reason, patients with high plasma Aldo content as in Primary Aldosteronism (PA) could have similar if not identical alterations as those evidenced in the inflammatory diseases described above.

The aim of this study was, at first, to ascertain if in PA RBCs were effectively altered as in other inflammatory diseases, and, then, to investigate how Aldo effects could induce eventual membrane alterations since a genomic way was to be ruled out in these cells and direct effect on enzymes such as protein kinases, phosphatases and structural protein have not yet been established in these cells.

MATERIALS AND METHODS

1. MATERIALS

Anti-phospho-tyrosine (P-Tyr) (PY20) mouse monoclonal antibody was obtained from Biosource-Invitrogen (Camarillo, CA, USA). The protease inhibitor cocktail and anti-actin mouse monoclonal antibody came from Calbiochem (Darmstadt, Germany). Anti-mouse, anti-rabbit and anti-sheep secondary antibodies conjugated with horseradish peroxidase (HRP) were obtained from Merck Millipore (Darmstadt, Germany).

Anti-Carbonic Anhydrase (CA) 2 cross reacting also with CA1 sheep polyclonal antibody was obtained from Abcam (Cambridge, United Kingdom). Anti-GSH was obtained from Virogen (Watertown, MA USA).

Antibodies anti-SHP2, anti-HSP90 and anti-GAPDH were purchased from Santa-Cruz Biotechnology, Inc. (CA, USA); anti-Syk and anti-phospho-Src (Tyr416) came from Millipore (Temecula, CA, USA).

Antibody anti-MR (MCR H-300), raised against aminoacids 1-300 of the C-terminal region of MR was purchased from Santa-Cruz Biotechnology, Inc.; anti-MR (MA 1-620), produced with aldosterone-3 as immunogen, came from Thermo Scientific (Rockford, IL, USA); protein prestained standards from Bio-Rad (Milan, Italy). Anti-band 3 antibody, molecular weight markers and any other reagents were purchased from Sigma (Milan, Italy).

2. STUDY PROTOCOL

Twenty-two untreated patients affected by PA by serum Aldo levels (intra- and inter-assay variations 5.3% and 7.0 %), aldosterone/renin ratio (ARR) and plasma renin activity (PRA) and 12 (6 males and 6 females) healthy volunteers as control

(HC) were enrolled at the Department of Medicine - Endocrinology of the University of Padova, Italy.

Diagnosis of PA was defined by the presence of aldosterone-renin ratio (ARR) > 30 (ng/dL)/(ng/mL/h), the lack of aldosterone suppression (<5 ng/dL) following an intravenous saline load (2 L of 0.9% saline infused over 4 hours) and the persistence of ARR > 30 (ng/dL)/(ng/mL/h) 90 minutes after the administration of 50 mg of captopril orally. Every patient underwent also an adrenal computed tomography (CT) scan and an adrenal venous sampling for subtype classification of PA. Before the study, all patients had stopped anti-hypertensive drugs interfering with the renin-angiotensin-aldosterone system for 4 weeks. The anti-hypertensive therapy was switched to an alpha-blocker (doxazosin) and/or calcium channel blocker (amlodipine). Patients with hypokalemia have continued with oral potassium supplementation. All the subjects were following an unrestricted normocaloric diet and undertook a normal physical activity; their sodium intake was not restricted and it was calculated at about 150 mmol/day.

None of the patients were affected by chronic inflammatory disease.

Parameter	**Normal range**	**PA Patients (*n*=22)**
Age (yr)	-	55.4±11.3
BMI (kg/m²)	-	27.5±3.4
Blood pressure (mmHg)		
Systolic	<120	155.3 ± 14.1
Diastolic	<80	97.5± 13.2
Sodium (mEq/L)	135-145	141.9±1.9
Potassium (mEq/L)	3.5-4.5	3.3±0.5
Aldosterone (ng/dL)	3.5-30	44.1±12
PRA (ug/L/h)	1.3-5.2	0.7±0.3
ARR	< 30	123.4±66.5

Table 1. Baseline clinical characteristics and haematochemical parameters of PA patients. Data are means ±SD.

At study entry, blood samples were collected from each subject to measure sodium, potassium, serum Aldo and PRA in upright position. Citrated blood samples were also collected for experimental procedures. During the same visit, anthropometric (weight, height and body mass index (BMI)) and clinical (heart rate, systolic and diastolic blood pressure) measurements were taken for all subjects. Clinical characteristics and biochemical parameters determined in the group of PA patients are listed in the Table 1.The Ethics Committee for Research and Clinical Trials of our University was notified and all participants gave their informed written consent prior to sample collection, according to the Declaration of Helsinki.

3. METHODS

3.1. Treatment of RBCs

Fresh blood, collected from patients and healthy volunteers, was centrifuged at 3750×g for 3 min.

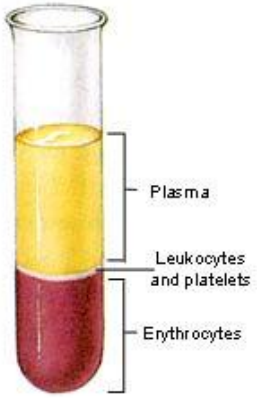

After removal of supernatant, packed RBC were washed three times at 3750×g for 3 min in 5 volumes of Dulbecco's Phosphate Buffered Saline (D-PBS). Packed cells (50 µl) were resuspended (at 20% hematocrit) in D-PBS and treated at 35°C for 30 min in absence ($_{Basal}$) or presence ($_{Diamide}$) of 1.5 mM diamide (dissolved in D-PBS) (Bordin et al., 2005b; Bordin et al., 2010b; Donà et al., 2012).

When the effect of Aldo was evaluated *in vitro,* only blood from HCs (n=12) was centrifuged at 3750×g for 3 min and plasma, not contaminated by leukocytes, was

further centrifuged at 1000×g for 20 min to obtain platelet-poor plasma (PPP) (Bordin et al., 2013). In order to remove small molecular weight macromolecules such as steroid and peptide hormones, dextran-coated charcoal was prepared (Bordin et al., 2013) by adding 500 mg of charcoal into the solution containing 50 mg of dextran and 100 mL D-PBS. The dextran-coated charcoal, or an equal volume of the same solution containing only dextran as control, was mixed with PPP (1:1). After stirring overnight at 4^{o}C, charcoal was removed by centrifugation and the Charcoal-stripped (CS-PPP) and unstripped (PPP) were obtained. The following day fresh RBC were obtained by the same volunteers who underwent a second blood sampling and RBC were purified as described above. RBC were washed three times in D-PBS as described above and packed cells were pre-incubated at 37^{o}C for 1 or 24h with PPP or CS-PPP at 20% hematocrit in absence (C) or presence of increasing concentrations of aldosterone (Aldo) with or without 1 μM canrenone (Can) or 5 μM cortisol (Cort) for 1h at 37°C. Stock solutions of 500 μM Aldo and Can were prepared in ethanol and further diluted in D-PBS to 500 nM and 50 μM, respectively, before use.

At the end of pre-incubation, samples were further incubated in the presence or absence of 1.5 mM diamide for 30 min and then recovered by centrifuging at 800×g for 3 min.

An aliquot of each sample was successively hemolysed in 30 volumes of hypotonic buffer (5 mM sodium phosphate, pH 8, 0.02 % sodium azide, 1 mM sodium orthovanadate, and a protease inhibitor cocktail). Membranes were separated from the cytosol by centrifugation (16100×g for 20 min in an Eppendorf centrifuge) and washed once in hypotonic buffer.

Both cytosol and membranes were submitted to sodium dodecyl sulfate-polyacrylamide gel electrophoresis (SDS-PAGE) and Western blotting, immunostained with the appropriate antibodies and bands were densitometrically scanned.

3.2. SDS-PAGE

Aliquots of membranes (10 µg) or cytosol were submitted to SDS-PAGE (8% gels). Samples were diluted into suitable quantity of sample buffer (2.5% SDS, 10% glycerol, 0.004% pyronin) and reduced/denaturated by heating to 100°C for 5 min with 1 M β-mercaptoethanol before run. When required, β-mercaptoethanol was avoided to analyze samples in non-reducing conditions. Separation was performed at constant current (50 mA) in running buffer (50 mM Tris-HCl pH 8.4, 0.38 M glycine, 5mM EDTA, 3.4 mM SDS in H2O).

3.3. Western blotting and immuno-detection

Gel-separated samples were electro-transferred on nitrocellulose membrane at 350 mA constant current for 2 h and 30 min into blotting buffer (25 mM Tris-HCl, 192 mM glycine, 20% v/v methanol and SDS 0.1%, pH 8.0). Immunological detection was then performed using appropriate primary antibodies and HRP-conjugated anti-rabbit and anti-mouse secondary antibodies. All washes were done with washing buffer (Tris-HCl 50 mM, pH 7.5, NaCl 150 mM, Tween 0.1%), saturation with Tris-HCl 50 mM, pH 7.5, NaCl 150 mM, bovine serum albumin (BSA) 3% and antibodies were diluted with Tris-HCl 50 mM, pH 7.5, NaCl 150 mM, BSA 1%.

Detection was done with freshly prepared solution by Amersham and densitometric analysis of immunoblots was obtained by the Image Station 4000 MM PRO (KODAK).

3.4. Determination of parameter variation

Band 3 variation ($V_{Tyr\text{-}P}$): Band 3 Tyr-P levels were evaluated densitometrically. The Tyr-P value of diamide-treated RBC from PA patients or Aldo-treated samples (**Tyr-Px**) was calculated as the ratio to the **$Tyr\text{-}P_C$**, i.e. Tyr-P level of diamide-treated RBC obtained in HC or in PPP 0 (0 nM Aldo) or in CS-PPP 0 (chosen as arbitrary comparison unit, experimentally determined as value±SD), according to the following formula:

$\mathbf{V_{Tyr\text{-}P} = (Tyr\text{-}P_X/Tyr\text{-}P_C)\text{-}1.}$

HMWA variation (V_{HMWA}): membranes (1 μg), were analysed by SDS-PAGE (8%) in non-reducing conditions, immunostained with anti-band 3 antibody and bands were densitometrically scanned. Amount of band 3 HMWA in control cells (HC or in unstimulated conditions) was chosen as arbitrary unit. Results represent means ± SD of six separate experiments in duplicate. The formula for $\mathbf{V_{HMWA}}$ calculation was:

$\mathbf{V_{HMWA} = (HMWA_X/HMWA_C)\text{-}1}$

IgG variation (V_{IgG}): membranes (8 μg) from diamide-untreated RBC were analysed by SDS-PAGE (8%), immunostained with anti-human IgG antibody and bands were densitometrically scanned. Amount of IgG in control cells (IgG_C) was chosen as arbitrary unit. Results represent means ± SD of six separate experiments in duplicate. IgG variation ($\mathbf{V_{IgG}}$) was obtained with the formula:

$\mathbf{V_{IgG} = (IgGx/IgGc)\text{-}1.}$

3.5. Glycerol gradient sedimentation

Aliquots of 300 μl of cytosol were loaded on a 3.9 ml glycerol (10%-40%) linear gradient in 25 mM N-2-hydroxyethylpiperazine-N′-2-ethanesulfonic acid, pH 7.4, 1 mM ethylenediaminetetraacetic acid. The tubes were centrifuged 18 hours at 100 000×*g* in an SW60Ti rotor (Beckman Coulter, Fullerton, CA) at 4°C and fractionated from the top into 18 fractions, and subjected to Western blotting analysis under denaturing conditions. Sedimentation markers run in parallel was formed by albumin (66 kDa), alcohol dehydrogenase (150 kDa) and β–amylase (200 kDa), apoferritin (443 kDa).

3.6. Anti-MR immunoprecipitations (IP)

Cytosol from untreated RBCs, obtained as described above was precleared with protein A-Sepharose, and then incubated for 5 h at 4°C with anti-MR antibody

bound to protein A-Sepharose. Immune complexes were washed three times in 50 mM Tris–HCl pH 7.5, 1 mM vanadate and protease inhibitor cocktail, and subjected to Western blot analysis by immunostaining with anti-MR antibody (Santa Cruz).

3.7. Anti-MR evaluation at confocal microscopy

Aliquots of untreated purified RBCs were washed with PBS, fixed with 2% (w/v) paraformaldehyde and incubated on slides pre-coated with poly-L-lysine. Slides were rinsed twice with PBS, treated with Triton X-100 and incubated with anti-MR in a humid chamber. Slides were washed three times with PBS, stained with anti-rabbit IgG- Tetramethyl Rhodamine Isothiocyanate (TRITC) conjugate in a humid chamber in the dark and mounted. Fluorescence was detected with the UltraView LCI confocal system (Perkin Elmer, Waltham, MA, USA). Staining without primary antibody was used as negative control.

3.8. Quantitative determination of total glutathione content in RBCs cytosol

Total glutathione in cytosol was determined according to the Tietze method (Tietze, 1979). Briefly, 10 μl of cytosol from HC and PA RBCs or from *in vitro* samples, were added to 2 ml of reaction mixture containing 1.9 ml of phosphate 0.1 M/ EDTA 0.6 mM buffer, pH 7.4, 30 μl of 5,5'-dithio-bis(2nitrobenzoic acid) (DTNB) 10 mM, 100 μl of NADPH 5 mM. After a 3 min equilibration period at room temperature, the reaction was started by the addition of 10 μg glutathione reductase (GR). Product formation was recorded spectrophotometrically at 412 nm, for 4 min at room temperature.

To assess any impairment in the antioxidant capacity of the erythrocytes, we treated RBCs of HC, PA or *in vitro* samples with diamide, and analysed cytosol glutathione content.

Previous study (Bordin et al., 2010b) demonstrated that after diamide treatment total glutathione in RBCs of patients with oxidative stress, dropped considerably

but did not significantly change in healthy controls. This suggested the hypothesis that the drop in total glutathione in patients was due to irreversible oxidation of glutathione, which remains bound to another protein, forming permanent disulphide bonds that GR could affect with minor efficacy.

For this reason we calculated the total decrease in glutathione content after diamide treatment (ΔGSH), expressed as **$1-(GSH_{(D)}/GSH_{(B)})$**, $GSH_{(D)}$ being change of absorbance in the sample with diamide treatment and $GSH_{(B)}$ that in untreated cells.

3.9. Determination of glutathione-protein mixed disulphide (GSSP) in RBCs

GSSP determination was carried out as previously described (Di Simplicio et al., 1998). Briefly, membranes, obtained as described above, were deproteinized by the addition of trichloroacetic acid (TCA) (5% final concentration) and kept on ice for 3 min. After centrifugation for 3 min at 16100×g, the pellet was resuspended with 0.4 ml basic solution containing 9 vol 0.1 M phosphate buffer (pH 7.4) and 1 vol 0.25 N NaOH, and stirred for 30 min at room temperature. Thirty microliters of 60% TCA was then added to cause precipitation and the amount of released GSH was determined enzymatically in the supernatant of centrifuged samples (as described above). Under these conditions thiols bound by mixed disulfides are easily removed.

The increase in glutathione released from membranes of RBCs after diamide treatment (D), representative of the increase in glutathionylated protein content (ΔGSSP), was expressed as (**$GSSP_{(D)}/GSSP_{(B)})-1$**.

3.10. Esterase activity assay

The activity of carbonic anhydrase was assayed by following the change in absorbance at 348 nm of 4-nitrophenylacetate (NPA) to 4-nitrophenylate (PNP) ion over a period of 10 min at 25 °C with a spectrophotometer (CHEBIOS UV–VIS) according to the method described by Verpoorte (Verpoorte et al., 1967).

Briefly, the enzymatic reaction was carried out in a total volume of 3.0 mL, containing 1.4 mL 0.05 M Tris–SO_4 buffer (pH 7.4), 1 mL 3 mM NPA, 0.5 mL H_2O and 0.1 mL diluted cytosol. A reference measurement was obtained by preparing the same cuvette with sample solution in the absence of incubation.
One unit of CA activity was defined as the amount of enzyme which catalyses the formation of 1 pmol PNP/min in standard conditions of incubation. The mixture was incubated for 10 min at room temperature, and the following formula incorporating the extinction coefficient was used to calculate: CA units $x10^{-3}$/ µl packed RBCs = OD × sample dilution factor /(min × 667), with an extinction coefficient of 667.

3.11. Tyr-protein kinase activity assays

Tyr-phosphorylation assays of membrane proteins were performed by incubating RBCs membranes (10 µg) for 10 min at 30ºC in 30-µl reaction mixtures containing 50 mM Tris–HCl, pH 7.5, 10 mM $MnCl_2$, 20 µM [γ-^{33}P]ATP (3×10^6 cpm/nmol) and 0.1 mM vanadate and 200 µM cdc2 peptide, which served as specific substrates for Src family tyrosine kinases. Reactions were stopped by the addition of 2% SDS and 1% β-mercaptoethanol (final concentrations) incubated for 5 min at 100ºC, and analyzed by SDS- PAGE and revealed by a Cyclone Storage Phosphor Imager. (Tibaldi et al., 2008)

3.12. Tyr-protein phosphatase activity assays

Phosphatase activity was measured at 30°C using 10 nM nitrophenyl phosphate (pNPP) as substrate in 100 mM tris-HCl (pH 7.4), 150 mM NaCl, 1 mM EDTA, 1 mM 2-mercaptoethanol, and samples membranes (10 µg). After 10 min at 30°C, the reaction was quenched with 950 µl of 1 M NaOH. Absorbance at 405 nm was measured. Results are expressed as percentage of activity compared to the controls.

3.13. Statistical analysis

Data are expressed as means ± SD. Comparisons were obtained with Student's t-test and statistical significance was set at $p<0.05$ (two-tailed). Any relationships between pairs of variables were tested by least-squares linear regression. Pearson's correlation coefficient r was used to quantify the strength of the relationships. The statistical significance of *r* was determined by ANOVA; a *p* value of less than 0.05 was considered statistically significant (two-tailed). Comparison between the slope of regression lines was performed with Student's t-test.

RESULTS

1. PART 1: identification and characterization of the RBCs alterations in PA patients

1.1. Evaluation of Band 3 Tyr-P level and HMWA content in PA patients

To examine RBCs membrane status, diamide-related band 3 Tyr-P levels were determined in patients' RBCs. Although in the absence of diamide stimulation Tyr-P could not be detected in RBCs from either controls or patients (Fig. 1A, lanes a, b), when PA RBCs were incubated with diamide, membranes showed higher band 3 Tyr-P levels in comparison with RBCs from HCs (Fig. 1A, lane d compared with lane c).

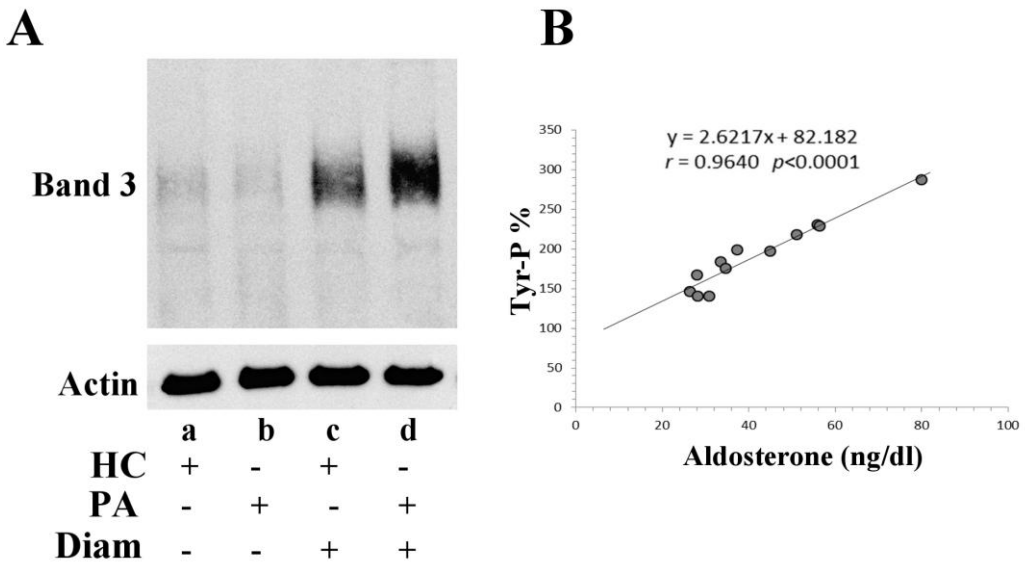

Figure 1. Panel A: Tyr levels in healthy controls (HCs) (lanes a, c) and in patients with primary aldosteronism (PA) (lanes b, d). RBCs, isolated as described in Methods, were incubated in the absence (lanes a, b) or presence (lanes c, d) of 1.5 mM diamide. Membranes, obtained as described in Methods, underwent Western blotting and were

immunostained with anti-P-Tyr, or anti-actin antibodies as a loading control. The figure is representative of more than 12 separate experiments.
Panel B: Linear regression between plasma Aldo and the band 3 Tyr-P level (after diamide treatment) (C) or HMWA formation (in the absence or presence of diamide treatment) (D). The Tyr-P value of diamide-treated RBC was calculated as the ratio to the Tyr-P level of diamide-treated RBC obtained in HCs (chosen as arbitrary comparison unit, experimentally determined as 99±2 mean value±SD).

Due to the wide range of the values obtained by the densitometrical evaluation of the band 3 Tyr-P levels in PA RBCs (Fig. 1A, Tyr-P increase of 93±43 %, $p<0.001$), we analyzed PA patients on the basis of their Aldo plasma level and a significant correlation ($r=0.9640$, $p<0.0001$) was found between plasma content of Aldo and band 3 Tyr-P level (Fig. 1B).

This Aldo-related increased response to diamide was further investigated by analyzing RBCs membrane status. Band 3 aggregates in high molecular weight (HMWA) complexes in a way that is directly dependent to the redox state of the cells (Bordin et al., 2010a; Bordin et al., 2006).

In Fig. 2 we reported band 3 HMWA pattern of membranes from PA patients (panel A, lanes a, b) and HCs (lanes c, d). Interestingly, PA patients (lane a) clearly showed higher HMWA content compared to HCs (lane c), even in the absence of diamide. Diamide addition induced further aggregation of band 3 both in PA patients (lane b) and in HCs (lane d) as expected due to diamide-induced disulfide bond formation between cysteine residues of band 3 (Lutz et al., 1988).

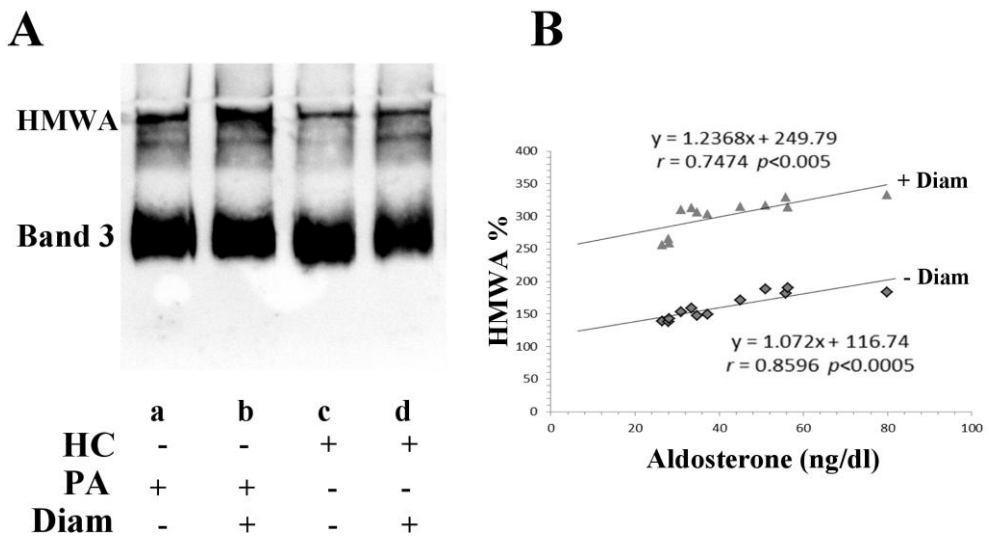

Figure 2. Panel A: Band 3 HMWA contents in PA patients (lanes a, b) and in HCs (lanes c, d). RBCs, isolated as described in Methods, were incubated with (lanes b, d) and without (lanes a, c) diamide. RBCs membranes, underwent Western blotting in non-reducing conditions, and were revealed with anti-band 3 antibodies. The figure is representative of 12 separate experiments.
Panel B: The HMWA values of both diamide treated (+Diam) and untreated (-Diam) RBCs from patients with PA were obtained as the ratio to the HMWA content of RBCs from HCs, respectively, in the presence or absence of diamide (chosen as arbitrary comparison units).

Upon densitometric analysis of HMWA content, a significant correlation with the plasma Aldo content of patients with PA (Figure 2B) was detected, both in the absence or in the presence of diamide (r=0.8596, p<0.0005 and r=0.7474, p<0.005, respectively). The slope of the 2 regression lines was not statistically different (p=0.6862), indicating that the 2 lines are parallel, thus confirming that both in the absence and presence of diamide, a similar correlation between plasma Aldo and HMWA content exists.

1.2. Evaluation of Aldo effects on Band 3 Tyr-P level and HMWA content in HC RBCs in in vitro treatments

To better evaluate whether the alterations seen in RBCs from patients with PA were due to increased plasma Aldo concentrations, we performed in vitro experiments with blood from HCs. As described in Methods, RBCs were pre-incubated for 1 hour or 24 hours at 35°C in CS-PPP or PPP with increasing Aldo concentrations, Can (1 µM), Cort (5 µM), both Aldo (5 nM) and Can (1 µM), or both Aldo (5 nM) and Cort (5 µM) and successively incubated in the presence or absence of 1.5 mM diamide. Membranes were analyzed by Western blotting with appropriate antibodies, and immunostained blots were evaluated densitometrically.

The band 3 Tyr-P level (Fig. 3) in RBCs pretreated in PPP 0 (0 nM Aldo), ie, in the absence of Aldo and other hormones, was chosen as a reference value for the PPP treatment and represented HCs conditions. Addition of increasing Aldo concentrations resembled RBCs environments in patients with PA. Can or Cort was added as an Aldo competitor. Samples incubated for 1 hour with PPP showed no detectable Tyr-P level in the absence of diamide. When added to PPP-pretreated RBCs, diamide triggered band 3 Tyr-P with an Aldo dose and time-dependent increase, peaking at 5 nM Aldo and rapidly decreasing at 10 nM, with a rise of band 3 Tyr-P ranging from 4±7 (1 hour) to 27±3 (24 hours) of band 3 Tyr-P variation ($V_{Tyr\text{-}P}$, see legend of Fig. 3), compared with the control (ie, in absence of Aldo). When RBCs pretreatment was performed with either Can or Cort in the absence of Aldo, band 3 Tyr-P level induced by diamide was not affected and remained at control levels. However, when pretreatment with Aldo (5 nM) was performed in the co-presence of Can or Cort, the consequent diamide-induced band 3 Tyr-P level was significantly reduced compared with the peak obtained with 5 nM Aldo ($V_{Tyr\text{-}P}$ of 8±3 and 3±3 for Can and Cort, respectively, at 24 hours).

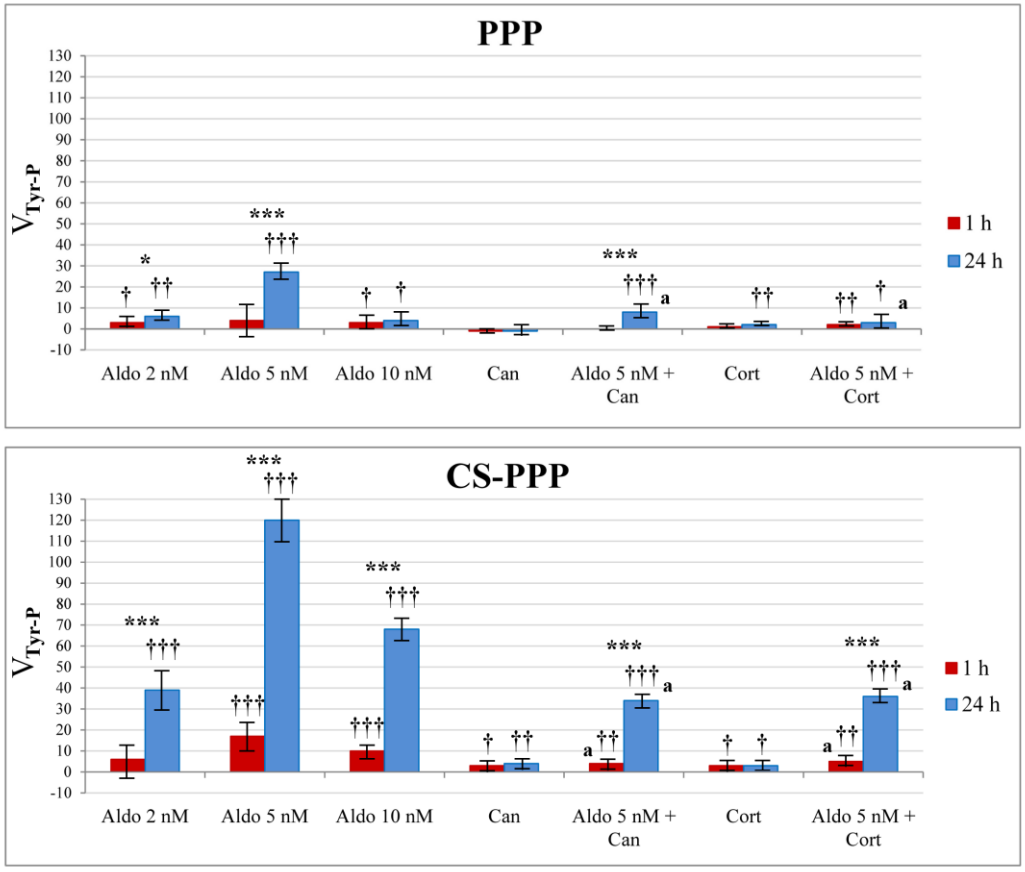

Figure 3. Effect of Aldo and 1 µM canrenone (Can) or 5 µM cortisol (Cort) on RBC Tyr-P in non-stripped (PPP) or charcoal-stripped (CS-PPP) plasmas at 1 and 24 hours of incubation. Data, expressed as variation compared with the respective controls in the absence of Aldo, Can, or Cort, are the mean±SD of 6 different experiments in duplicate. $V_{Tyr\text{-}P}$ is the band 3 Tyr-P variation, evaluated densitometrically. To better appreciate the variations obtained in different samples, we evaluated the Tyr-P level in relation to the corresponding controls (absence of Aldo). Therefore, the Tyr-P value of diamide-treated RBC from Aldo- Can-, and Cort-treated or co-treated samples ($Tyr\text{-}P_X$) was calculated as the ratio to the correspondent $Tyr\text{-}P_C$, ie, the Tyr-P level of diamide-treated RBCs obtained in PPP 0 (0 nM Aldo) or in CS-PPP 0, according to the following formula: $\mathbf{V_{Tyr\text{-}P} = (Tyr\text{-}P_X / Tyr\text{-}P_C) - 1}$.

* $p<0.05$; *** $p<0.001$, comparison between 1 and 24 hours.

† $p<0.05$; †† $p<0.01$; ††† $p<0.001$, comparison with the respective basal value (Aldo 0 nM).

a $p<0.001$, comparison of (5 nM Aldo) vs (5 nM Aldo+Can), or (5 nM Aldo) vs (5 nM Aldo+Cort), within each respective experimental condition.

To ascertain that the effects shown with Aldo pretreatment were effectively due to Aldo, we incubated RBCs in CS-PPP, ie, in plasma stripped of steroid hormones. Diamide addition to CS-PPP RBCs pretreated with increasing concentrations of

Aldo induced high Tyr-P, peaking at 5 nM and resembling those reported for patients with PA (Fig. 1B). In fact, 5 nM Aldo pretreatment-induced $V_{Tyr\text{-}P}$ was about 17±5 after 1 hour (p<0.001), but reached 120±10 after 24 hours (p<0.001) (Fig. 3). Interestingly, in this case also, further increasing the Aldo concentration to 10 nM induced a reduction in the extent of the Tyr-P level. When Aldo was replaced by Can or Cort, the diamide-induced band 3 Tyr-P level remained at the control level and when 5 nM Aldo was added in association with Can or Cort, diamide- P-Tyr levels were strongly reduced.

The HMWA content of RBCs incubated with Aldo in PPP in the absence of diamide reached an V_{HMWA} of 11±5 (at 1 hours) and 23±3 (at 24 hours), compared with the control (absence of Aldo pretreatment) (Fig. 4). Can or Cort did not induce any alteration in the above parameters, but when added with Aldo prevented Aldo-related effects. Interestingly, no decrease was shown by further increasing the Aldo concentration to 10 nM, either at 1 hour or 24. When HMWA formation was evaluated after CS-PPP pretreatment with increasing Aldo concentrations, a dose- and time-dependent effect of Aldo was seen, peaking at 5 nM with a maximal V_{HMWA} never exceeding 21±3 after 1 hour (p<0.001) and 63±3 after 24 hours (p<0.001) and followed by a slight decrease at 10 nM at both incubation times.

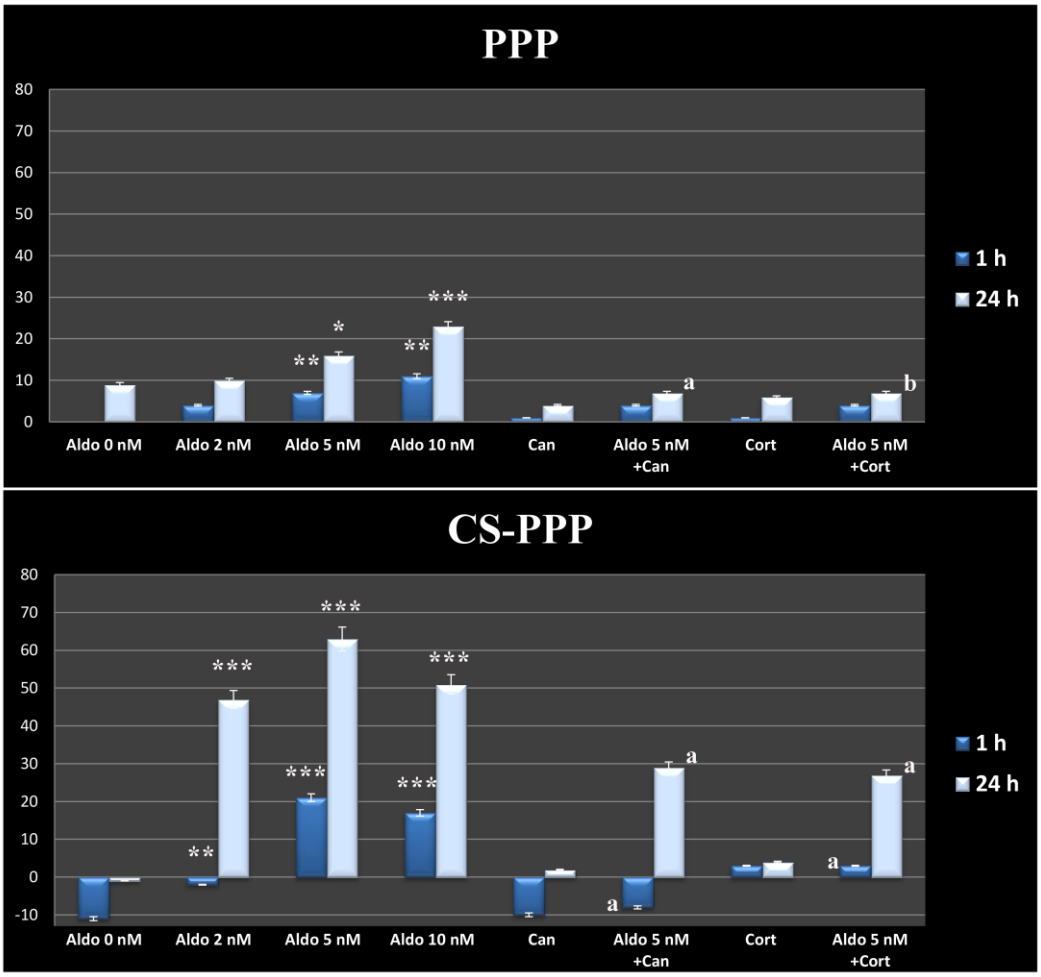

Figure 4. Effect of Aldo, 5 µM canrenone (Can) or 5 µM cortisol (Cort) on band 3 high molecular weight aggregates (HMWA) and IgG binding in in non-stripped (PPP) or charcoal-stripped (CS-PPP) plasmas. Data, expressed as variations compared with the respective control incubated in the absence of Aldo, Can, or Cort, are the means±SD of 6 different experiments in duplicate.

HMWA variation (V_{HMWA}): Membranes (1 µg) from RBCs treated for 1 hour or 24 hours with Aldo, 1 µM Can, or 5 µM Cort in PPP or CS-PPP, were analyzed by SDS-PAGE (8%) in non-reducing conditions and immunostained with anti-band 3 antibody and bands were scanned densitometrically. The amount of band 3 HMWAs in unstimulated conditions ($HMWA_C$: Aldo 0 in PPP, at 1 h) was arbitrarily chosen as unity. The formula for V_{HMWA} calculation was $\mathbf{V_{HMWA}=(HMWA_X/HMWA_C)-1}$.

* $p< 0.05$; ** $p< 0.01$; *** $p<0.001$, comparison with the respective basal value (0 nM Aldo).

b $p< 0.01$; **a** $p< 0.001$, comparison (5 nM Aldo) vs (5 nM Aldo+Can) or (5 nM Aldo) vs (5 nM Aldo+Cort), within each respective experimental condition.

To evaluate the possible involvement of Aldo pre-incubation in altering RBCs life span, membranes obtained from the samples described above were analyzed for

their IgG content (Fig. 5). In this case also, Aldo pretreatment induced a marked increase in autologous IgG binding, plateauing at 5 nM in both PPP and CS-PPP samples, which was completely prevented by Can or Cort co-addition.

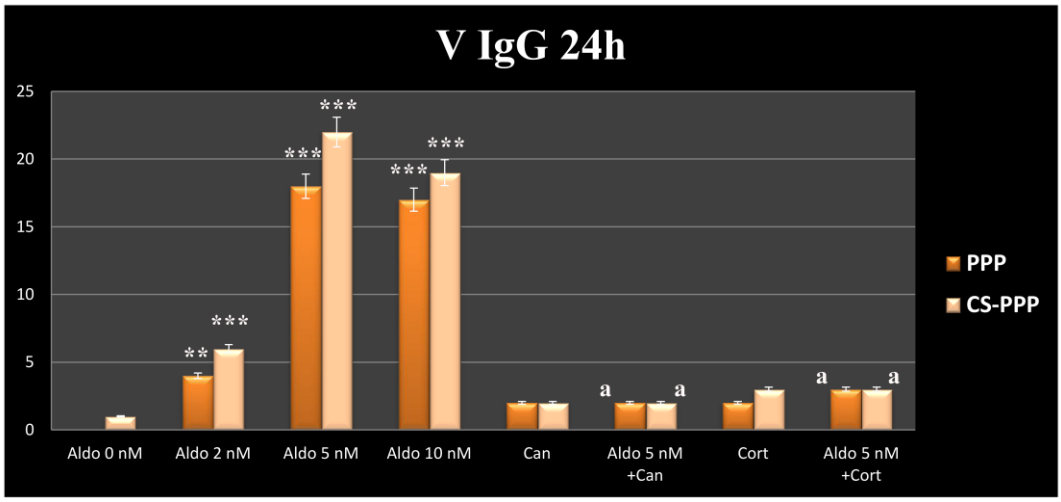

Figure 5. Effect of Aldo, 5 µM canrenone (Can) or 5 µM cortisol (Cort) on IgG binding in in non-stripped (PPP) or charcoal-stripped (CS-PPP) plasmas. Data, expressed as variations compared with the respective control incubated in the absence of Aldo, Can, or Cort, are the means±SD of 6 different experiments in duplicate.

IgG variation (V_{IgG}): Membranes (8 µg) from RBCs treated for 24 hours with Aldo, 5 µM Can, or 5 µM Cort in PPP or CS-PPP were analyzed by SDS-PAGE (8%) and immunostained with anti-human IgG antibody and bands were densitometrically scanned. The amount of IgG in Aldo 0 in PPP (IgG_C) was chosen as an arbitrary unit. V_{IgG} was obtained with the formula: $\mathbf{V_{IgG} = (IgG_X/IgG_C)-1}$.

** $p< 0.01$; *** $p<0.001$, comparison with the respective basal value (0 nM Aldo).

a $p< 0.001$, comparison (5 nM Aldo) vs (5 nM Aldo+Can) or (5 nM Aldo) vs (5 nM Aldo+Cort), within each respective experimental condition.

2. PART 2: ALDO-MR PATHWAY

2.1. MR detection in human RBCs cytosol

In the first part of the study it has been hypothesized that Aldo affected membranes through a pathway involving MR, due to the inhibitory effect of Can that almost completely prevented Aldo-induced membrane alterations. To investigate the presence of MR, both cytosol and membranes of HC RBCs were analyzed by Western blotting and revealed with anti-MR antibodies (Fig. 6, panel B).

Immunodetection showed bands at 100, 80, 50-53 and additional bands at 20-25 kDa in cytosol (lane b) but when membranes were analyzed, no trace was evident (lane a).

RBCs immunocytochemistry analysis with anti-MR (MCR H-300) antibodies revealed homogeneous diffuse fluorescence, confirming the presence of the receptor within the cell (panel A).

Due to the fact that the aggregation of steroid receptors in multiprotein complexes generally involves the chaperone protein HSP90 (Mjahed et al., 2012), we analyzed its potential presence in the cytosol of human RBCs. Immuno-blotting with anti-HSP90 antibodies confirmed that HSP90 was present in both cytosol (panel C, lane a) and, although partially proteolysed, also in membranes (lane b). Interestingly, anti-MR IP also exhibited a consistent band of anti-HSP90, co-immuno-precipitating with MR (lane c).

These results prompted us to separately investigate cytosol and membranes to better understand the mechanism of action and regulation of MR in the cytosol and the related pathway leading to membrane alterations.

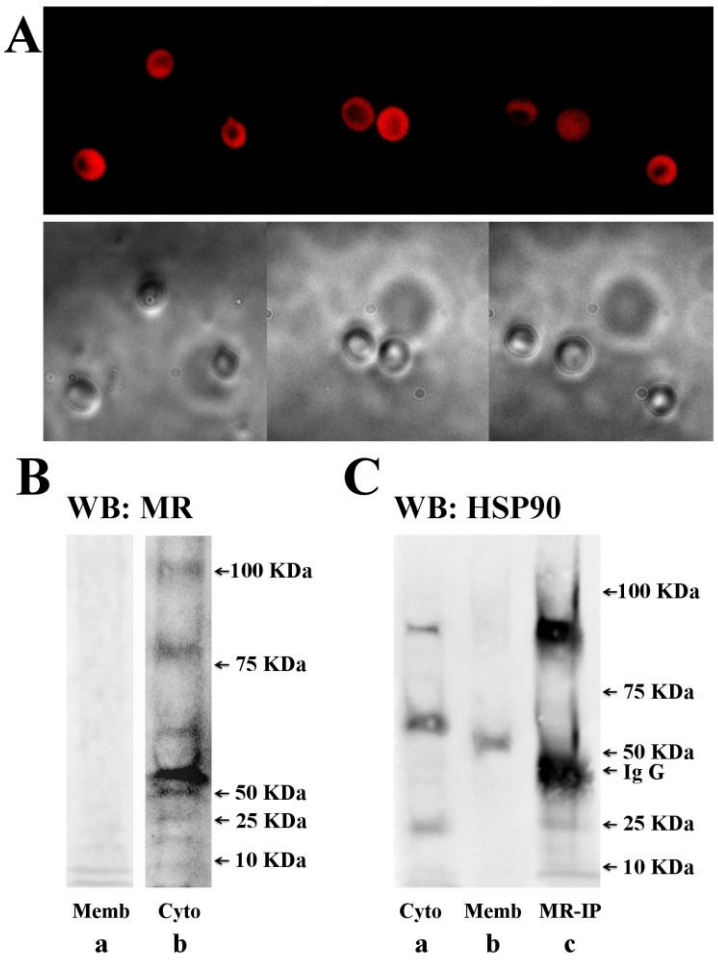

Figure 6. Identification and localization of mineralocorticoid receptor (MR) in human RBCs. Panel A: Anti-MR detection by immunofluorescence cytochemistry of untreated RBCs from healthy controls (HCs); corresponding phase-contrast images are shown. **Panel B: Anti-MR Western blotting.** Untreated RBCs from HCs, isolated as described in Methods, underwent haemolysis. Membranes (lane a) and cytosol (lane b) obtained as described in Methods, underwent Western blotting and were immunostained with anti-MR antibody**. Panel C**. **Anti-HSP90 Western blotting**. Cytosol (lane a), membranes (lane b) and anti-MR immunoprecipitate (MR-IP, lane c) obtained from cytosol were analysed by Western blotting and immunorevealed with anti HSP90 antibody. The figure is representative of five separate experiments.

2.2. MR gradient sedimentation in human RBCs cytosol: MR activation by Aldo

After RBCs hemolysis, cytosol was further processed by glycerol gradient sedimentation, and sedimentation profiles were analysed by Western blotting to

ascertain whether MR was present as a monomer or a dimer/polymer (Fig. 7). In the control C, RBCs cytosol immunodetection with anti-MR showed that MR was stratified into a large number of glycerol fractions, from 3 to 10, i.e., over a wide range of molecular weights, probably due to its interaction with other proteins. In addition, within each fraction, MR itself was present as different isoforms, simplified in two main regions: one, at 20-25 kDa (panel B) involved two bands which were more evident in fractions 4-6 (corresponding to glycerol sedimentation weight ranging from about 80 to 130 kDa); and the other involving bands from 50 to 80 kDa (panel A), visible only from fraction 5 to 10 (corresponding to the 100-400 kDa range of sedimentation weights). In fractions 5-7 only bands of 50-53 kDa were well distinguishable; in fractions 8-10, a new band at about 60 kDa appeared but those at 50-53 kDa disappeared (panel A, sample C).

The addition of 5 nM Aldo induced net rearrangement of the band at 60 kDa, which almost disappeared from fractions 8-10, whereas the 50-53 kDa band increased in fractions 4-9 (Fig. 7, panel A sample C compared with sample Aldo).

Concomitantly, Aldo also induced the appearance of the 80 kDa isoform in fractions 5-7 and shifting of the 20-25- kDa bands from fractions 4-6 in sample C to fractions 3-6 in sample Aldo (Fig. 7, panel B).

Surprisingly, when the same fractions were immuno-detected with anti-MR (MA 1-620) antibody produced with aldosterone-3 as immunogen, MR was detected only in fractions 6-10, whereas no trace was appreciable in the other fractions, in either C or Aldo samples (not shown). This discrepancy with MR (MCR H-300) detections (Fig. 7) suggests that Aldo-MR binding is not reversible since Aldo remains entrapped in the MR pocket even after MR proteolysis and the complex Aldo-MR is no longer detectable by MA 1-620 antibody, as indicated by the corresponding datasheet (not shown).

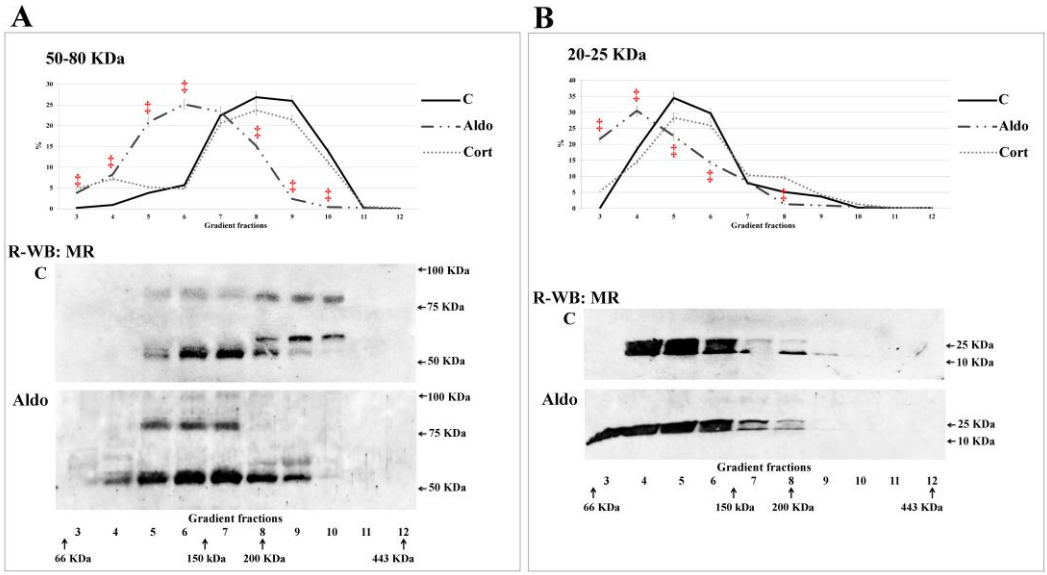

Figure 7. MR gradient sedimentation. RBCs from 12 healthy volunteers, purified as described in supplementary section methods, were incubated at 37°C for 1h in absence (C) or presence of 5 nM aldosterone (Aldo) or 5 µM cortisol (Cort) in charcoal-stripped plasma to remove small molecular weight macromolecules such as steroid and peptide hormones. Incubated RBCs were hemolysed and 300 µl of diluted cytosol was loaded on top of a linear glycerol gradient and centrifuged for 18 hours at 100 000×*g*. Eighteen fractions (200 µL each) were collected from top, analysed by Western blotting and immuno-detected with anti-MR antibody (MCR H-300) raised against aminoacids 1-300. **Panels A** and **B:** bands corresponding to 50-80- and 20-25-kDa regions of gels. Data are means ± SD of duplicate measurements from 12 healthy volunteers. Densitometric analysis of anti-MR Western blots of 50-80- and 20-25-kDa bands (panels A and B, top panels) were quantified; data are expressed as % of total amount of 50-80- or 20-25-kDa bands, respectively, in all fractions, according to $\mathbf{MR\text{-}bands_{fraction}/MR\text{-}bands_{total}}$.
Statistical analysis showed significant difference at peak values between control and Aldo conditions (‡ $p<0.0001$, ANOVA, comparison C *vs* Aldo).
Arrows at the bottom of panels: position of molecular weight standards on glycerol gradients, albumin (66 kDa), alcohol dehydrogenase (150 kDa), β-amylase (200kDa) and apoferritin (443 kDa), to estimate molecular weight of protein complexes on parallel gradient runs.

Densitometrical analysis of the bands in the 50-80 kDa region (panel A diagram) of C sample peaked in fractions 7-10. The same MR isoforms as in the Aldo sample (dotted lines) were shifted to fractions 5-8, whereas Cort did not induce any change in the location of the MR peak which remained similar to that of controls. These results showed that Aldo treatment induced MR to break away from the multiprotein complex, and MR dimers were formed, as indicated by the appearance of 80-kDa bands in the region of 90-170 kDa range of the gradient. In

addition, the increase in low molecular weight bands (20-25 kDa) in fractions 3-6 (panel B) showed the degradation of MR (again demonstrated by a shift of peak position) triggered by treatment with Aldo, but not by Cort.

The addition of Can, either alone or in association with Aldo, did not alter the MR situation, which was similar to that of controls (data not shown). Similar results were obtained when RBC were co-treated with Aldo and Cort (data not shown).

When Western blotted glycerol fractions were immuno-detected with anti-HSP90 antibodies, a major band at 90 kDa and a proteolysed isoform of about 60 kDa were mainly sedimented in fractions 6-10. Other treatments did not induce appreciable movements of trend-lines compared with controls (data not shown).

2.2.1. Effect of Aldo or Cort on MR fragmentation

The presence of low molecular bands (20-25 kDa) raised the possibility that a proteolytic process regulates the MR pathway. Low weight MR bands were collected in a large number of fractions (3-9), suggesting that the 20-25 kDa isoforms were both part of multi-complex proteins (fractions 8-10) or derived from a single monomer of MR (fractions 3-5). In addition, a band of less than 10 kDa was found in C samples from fractions 4-7, suggesting the occurrence of further proteolytic digestion mainly in the monomeric and dimeric forms of MR (data not shown).

Glycerol gradient fractions were thus analyzed by Western blotting in non-reducing conditions to highlight any fragments broken away from the multi-protein complex. Figure 8 compares the anti-MR patterns obtained with non-reducing (NR) Western blotting of Aldo- and Cort-treated samples. Anti-MR bands at 50-60 kDa, present in fractions 5-10 of reducing (R)-WB (Fig. 7, panels A), were no longer be detected, whereas two sets of bands were evidenced. The first showed a band at high molecular weight (HMW) which did not change in any of the conditions (data not shown) and the second set was composed by bands corresponding to 20-25 and < 10 kDa bands (Fig. 8, panels A and B). Aldo induced both the formation of bands in the region $\leq$ 25 kDa in fractions 3-4 and net shifting of bands <10 kDa to fractions 3-8. Cort did not affect the number of low- weight bands which remained at the level of controls (panel B).

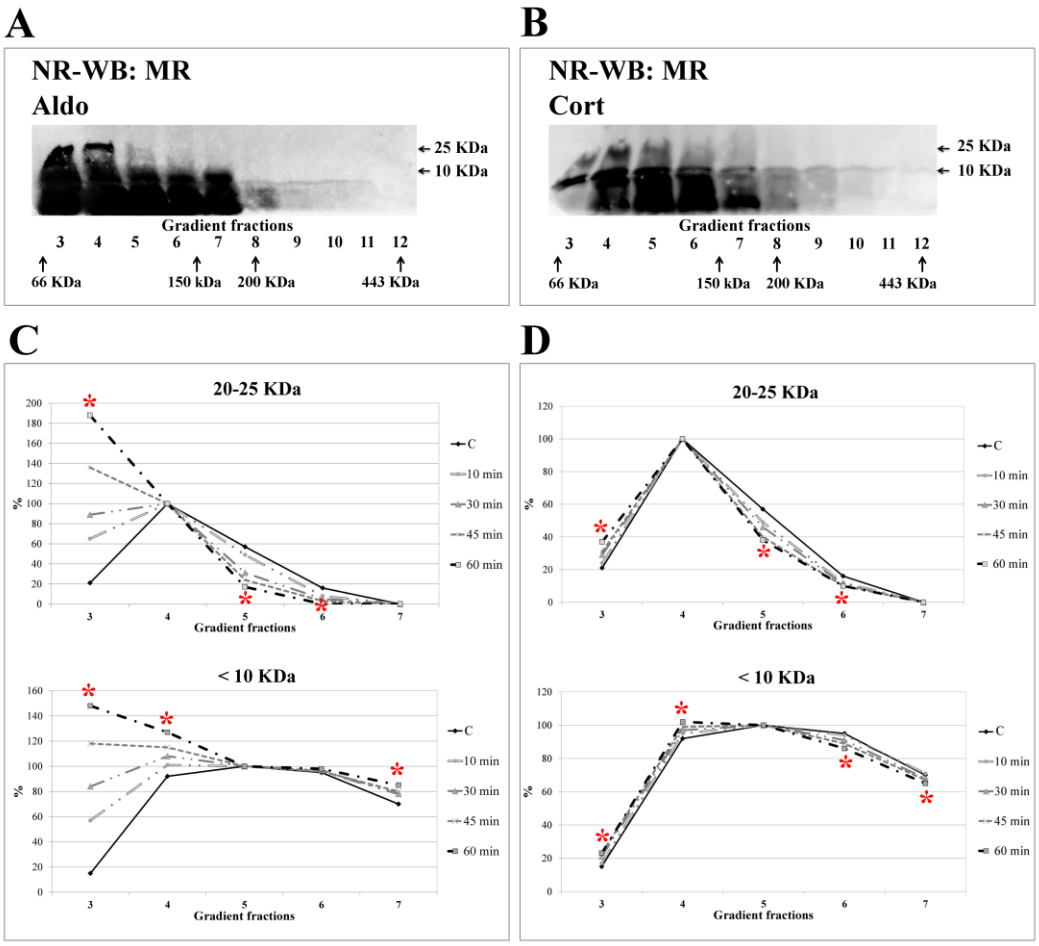

Figure 8. RBCs from 12 healthy volunteers, incubated at 37°C for increasing times (10, 30, 45, 60 min) in absence (C) or presence of 5 nM aldosterone (Aldo) or 5µM cortisol (Cort), were hemolysed and 300 µl of diluted cytosol were loaded on top of a linear glycerol gradient and centrifuged for 18 hours at 100 000×*g*. Fractions (200 µL each) from top were analysed by Western blotting in non-reducing conditions and immune-detected with anti-MR antibody. **Panels A** and **B**: bands corresponding to 20-25 and <10 kDa regions of gels of samples Aldo and Cort incubated for 60 min.
Panels C and **D:** values from samples incubated for increasing times with Aldo and Cort. Bands were densitometrically analysed and compared with corresponding controls: highest band in C for each molecular weight region was taken as comparison unit. Same fraction as in C containing highest band was considered as comparison in other samples.
*: values significantly different between C and 60-min curves (ANOVA, $p<0.001$).

The intriguing involvement of a proteolytic process degrading MR after addition of Aldo but not of Cort was further investigated in experiments carried out at increasing incubation times.

Samples were treated in the absence (C) or presence of Aldo or Cort for 10, 30, 45 and 60 min and cytosols were analyzed by glycerol gradient sedimentation. In the NR-WB of fractions MR bands corresponding to 20-25 and <10 kDa which were densitometrically evaluated and separately counted and reported in panels C (Aldo) and D (Cort). Aldo addition resulted in time-dependent MR fragmentation starting from the first 10 min of incubation in both 20-25 and <10 kDa regions. Interestingly, in the Cort-treated samples, MR only showed a slight shift to fraction 3 of the proteolytic fragments. When bands at 50-80 kDa were examined in R-WB (not shown) Cort induced a light shifting to fractions 3 and 4 in the first 10 min but, after 60 min MR bands were recovered in the same fractions as the control, as if re-adjustment of Cort-MR were compatible with re-aggregation of MR in the multi-protein complex. Conversely, Aldo effect confirmed a time-dependent shift to the first fractions.

2.2.2. MR association in multiprotein complexes

Further study of MR-multiprotein complex dissociation was carried out in the cytosol of untreated RBC and fractions 8-10 from the glycerol gradients were pooled. In these fractions, MR was part of the multi-protein complex and present in the highest isoforms (Fig. 7, panel A). The pooled fractions were then divided into five aliquots and treated at 0°C for 30 min in the absence (controls) (Fig. 9, panel A, lane a) or presence of 5 μM Cort (lane b), 1 μM Can (lane c), 2 or 5nM Aldo (lanes d and e) in order to allow the ligands to bind to the receptor, which was then immuno-precipitated by the addition of anti-MR. MR-immuno-precipitates (IP) from control- and Can- treated aliquots only showed traces of MR (lanes a, c), as revealed by WB with anti-MR antibody (MCR H-300). In the Cort-treated aliquot, the MR band was more than three times that of the control (+315% lane b *vs* lane a, $p<0.0001$) whereas Aldo treatment induced a dose-dependent decrease in the MR-IP band (-25 and -55%, lanes d and e, respectively, *vs* lane a, $p<0.0001$). To better characterize the complex ligand-receptor, supernatant recovered from the previous IP were re-immuno-precipitated (Re-IP) in the presence of DTT, a reducing agent, and immuno-detected with anti-MR

(panel B: Re-IP). The amount of MR recovered from Aldo-treated samples increased greatly compared with that recovered from the control (+30 and +60 % lanes d and e, *vs* lane a, $p<0.0001$), whereas from the Cor- treated sample the Re-IP MR band was -90% (lane b; $p<0.0001$) compared with controls. Re-IP from Can-treated samples yielded the same band as controls (lane c *vs* lane a).

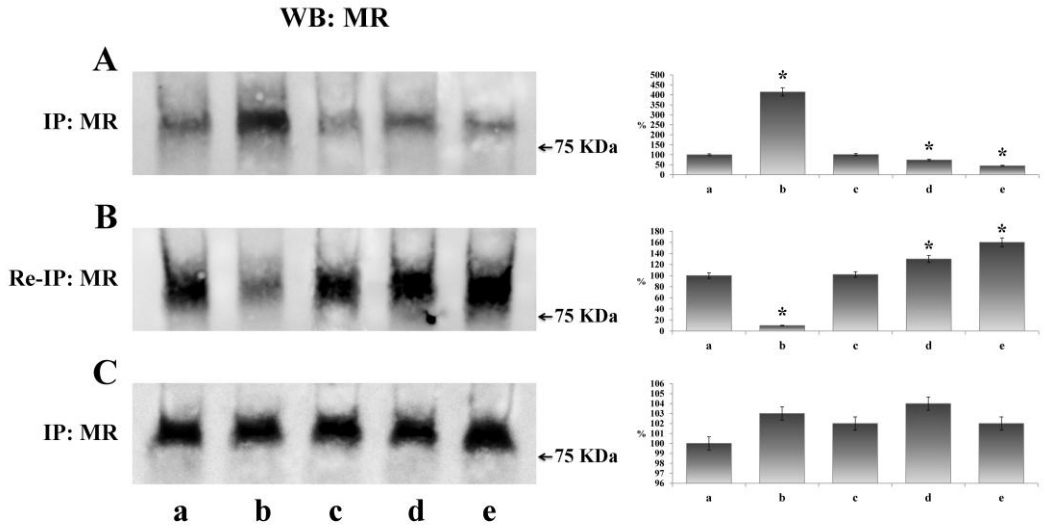

Figure 9. Fractions 8-10 from the C sample glycerol gradients were collected, divided into 5 aliquots and treated at 0°C for 30 min in absence (control) (lane a) or presence of 5 μM Cort (lane b), 1 μM Can (lane c), 2 or 5 nM Aldo (lanes d and e). **Panel A:** MR was then immunoprecipitated by anti-MR (MCR H-300) and MR-IPs were analysed by Western blotting with anti-MR antibody. **Panel B**: supernatants recovered after MR-IP as described above were re-immunoprecipitated in presence of 5 mM dithiothreitol (DTT) and MR-IPs were analysed by Western blotting with anti-MR antibody. **Panel C:** fractions 8-10 from C sample glycerol gradients were collected, divided into 5 aliquots and treated at 0°C for 30 min with Gelda 100 nM in absence (control) (lane a) or presence of 5 μM Cort (lane b), 1 μM Can (lane c), 2 or 5nM Aldo (lanes d and e). MR was then immunoprecipitated by anti-MR (MCR H-300) and MR-IPs were analysed by Western blotting with anti-MR antibody.Bands were densitometrically analysed and reported on the right of the corresponding panel.
* $p<0.0001$ *vs* control (lane a).

DTT induced increase in further MR re-immuno-precipitations from almost all samples, except Cort-treated ones, is due to the fact that the N terminal (1-300) region of MR, recognized by the antibody, was involved in dimer/complex formation, thus preventing MR immuno-precipitation. The decrease of MR-IP in Aldo-treated samples was due to Aldo-MR dimer formation, as shown by the

shifting of the MR-recovering curve in glycerol gradient sedimentation (Fig. 7). In the MR dimer, binding was more stable than in the complex (Fig. 9, lane a), meaning that the antibody was less capable of recognizing the N-terminal region compared with controls. Instead, Cort treatment induced MR release from the complex but not dimer formation, thus making the MR-N-terminus recognizable by the antibody. Reducing conditions may dissociate MR from both dimer and complex, as indicated by the increase in the MR-band in Re-IP assays of controls and Aldo-treated samples (Fig. 9, panel B, lanes a, d, e). Can did not alter the structure of the MR-complex, which remained at control level.

For further confirmation, the addition of Geldanamycin (Gelda), an apoptotic compound which inhibits HSP90 and disrupts the cytosol-multiprotein complex (Stebbins et al., 1997), prevented Aldo-induced dimer formation, as demonstrated by complete recovery of MR from all samples (panel C, lanes a-e) and the absence of MR in the Re-IP assay in reducing conditions (data not shown).

2.2.3. MR-complex involvement in Aldo signaling

When HC RBCs were pre-incubated in CS-PPP in the presence of Geldanamycin and successively incubated with Aldo, both HMWA formation (data not shown) and IgG binding were completely prevented (Fig. 10, lane e compared to lane d), thus confirming the involvement of HSP90 in the maintaining the correct MR conformation for Aldo binding and the successive MR activation.

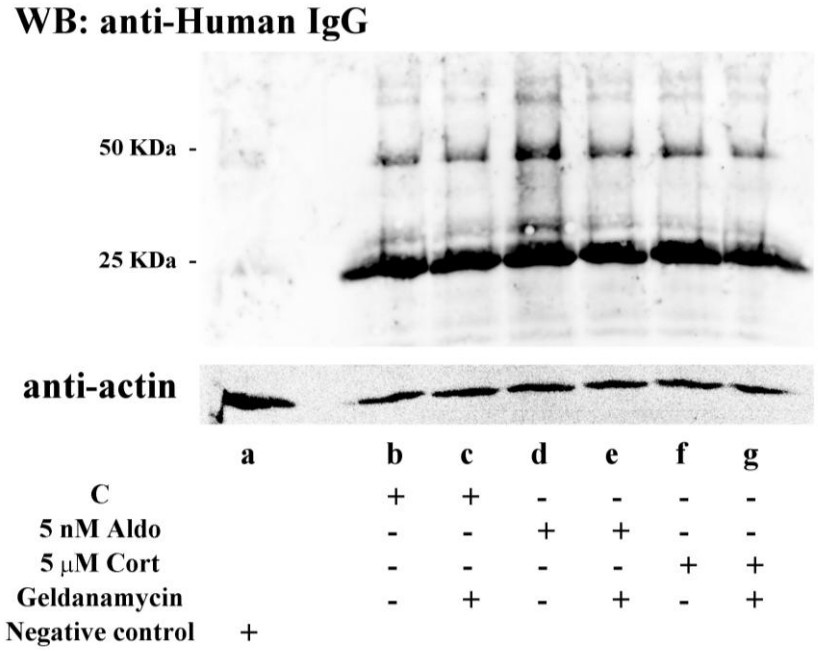

Fig. 10. IgG binding to RBCs membrane. HC RBCs were pre-incubated (20 min at 37°C) in CS-PPP in absence (lanes b, d and f) or presence of Geldanamycin (lanes c, e and g) and successively incubated at 37°C for 1 h, without (lanes b and c) or with 5 nM Aldo (lanes d and e) or 5 μM Cort (lanes f and g). After incubation, all samples were haemolysed in hypotonic buffer. Membranes of HC RBCs, washed and haemolysed without incubation, were used as negative control (lane a). RBCs membranes (2 μg), obtained as described in Methods, were then analysed by SDS-PAGE (8%) and immunostained with anti-Human IgG antibody and anti-actin, as loading control.

3. PART 3: Partial characterization of the Aldo-induced alterations in PA RBCs

3.1. Parameters of the cellular oxidative status

Due to the evidence that Aldo induced membrane alterations leading to band 3 HMWA formation and diamide-induced high Tyr-P level are similar to those previously reported in inflammatory related increased oxidative stress conditions (Bordin et al., 2010b; Donà et al., 2012), HC and PA RBCs membranes were analysed by Western blotting and immuno-revealed with anti-GSH antibody (Fig. 11 and Table 1). Significantly, no difference was evident between PA and HC RBCs membranes.

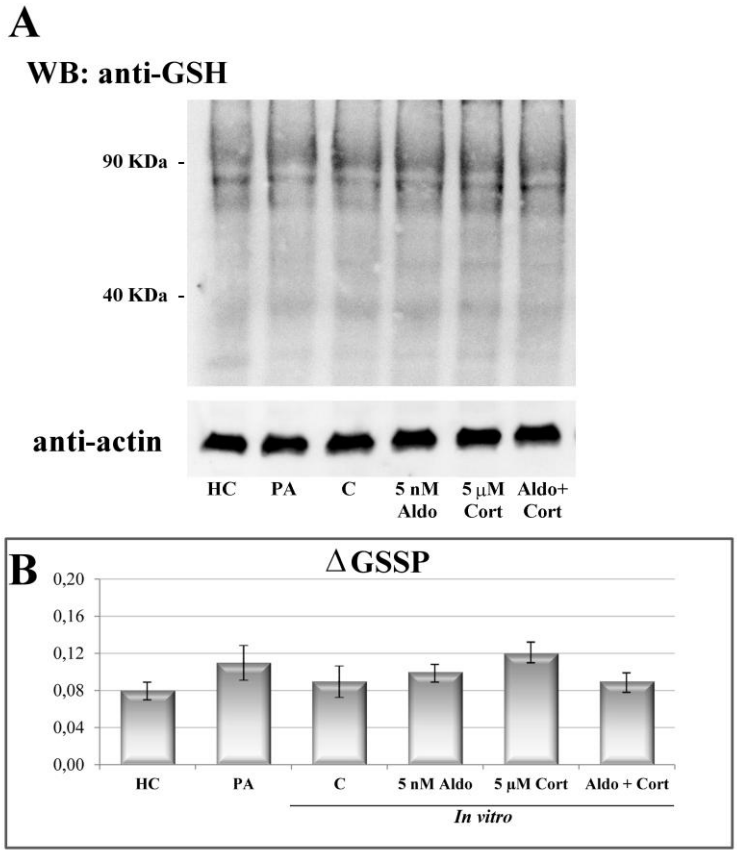

Figure 11. Panel A: GSH in RBCs membrane from HC, PA and *In vitro* samples. RBCs were isolated from fresh blood collected from controls (HC) (n=12) and patients (PA) (n=22) and isolated as described in Methods. For *in vitro* treatment, only blood from

HC was utilized, and RBCs, were incubated at 37°C for 1h in absence (C) or presence of 5 nM aldosterone (Aldo) or 5 μM cortisol (Cort) or both (Aldo+Cort), in charcoal-stripped plasma to remove small molecular weight macromolecules such as steroid and peptide hormones. Membranes (10 μg), obtained as described in Methods, underwent Western blotting in non-reducing conditions and were immunostained with anti-GSH antibody, or anti-actin antibody as loading control. Figure is representative of the study population.

Panel B: Determination of glutathione-protein mixed disulfide (GSSP) in RBCs. Membranes, obtained from HC, PA and *In vitro* samples (C, Aldo, Cort and Aldo+Cort) as described in Methods, were TCA-deproteinized and alkalinized, and the amount of GSH released from proteins was determined enzymatically in the supernatants, as described in Methods.

The increase in glutathione released from RBCs membranes after diamide (1.5 mM) treatment, representing increase in glutathionylated protein content (ΔGSSP), is expressed as $(GSSP_{(D)}/GSSP_{(B)})$-1.

Data show the means ±SD. Comparison HC *vs* PA and for in vitro experiments, C *vs* Aldo, Cort and Aldo+Cort. Student's *t* test reveals no statistical significance.

This result was further investigated by extracting the total glutathione bound to the membrane proteins (GSSP). No detectable difference in the content of GSSP was present between the two groups. Diamide treatment has been shown to emphasize eventual pre-existent alterations related to an enhanced oxidative status by increasing the amount of GSH irreversibly bound to membranes (Donà et al., 2012; Andrisani et al., 2014). The difference between GSH contents in the absence and presence of diamide (ΔGSSP) was representative of the redox state of membranes (Donà et al., 2012). When analysed for ΔGSSP, no variation in the content of GSH bound to membrane proteins was evidenced, thus confirming that both HC and PA membranes shared the same redox conditions (Table 1). Concomitantly GSH content was evaluated also in the cytosol in absence and presence of diamide, and the relative ΔGSH calculated. Also cytosol showed no alteration in the redox state (Table 1).

To characterize the effect of Aldo while avoiding the potential interference of other circulating steroid hormones, plasma was treated overnight with charcoal, which can bind and strip steroids and other small molecules (Bordin et al., 2013). RBCs were then pre-incubated for 1h at 37°C in charcoal-stripped (CS-PPP) plasma with 5 nM Aldo, 5 μM Cort, 1 μM Can, alone or in association (Aldo and

Cort, or Aldo and Can), and cytosol and membranes recovered as described in Methods.

As indicated in Table 1, also in *in vitro* experiments, Aldo did not induce any increase in protein glutathionylation of membrane, nor in the redox state as indicated by the ΔGSSP (Donà et al., 2012). When cytosol was analysed for GSH and GSSG content, no alteration was induced by Aldo treatment, thus confirming that Aldo-induced alterations were not mediated by oxidative assault involving GSH dependent defense.

	Samples	ΔGSH	ΔGSSP
	HC	0.09±0.03	0.08±0.03
	PA	0.11±0.02	0.1±0.03
In vitro	**C**	0.1±0.04	0.09±0.04
	2 nM Aldo	0.08±0.03	0.12±0.02
	5 nM Aldo	0.09±0.02	0.11±0.02
	5 µM Cort	0.11±0.02	0.08±0.04
	Aldo + Cort	0.08±0.04	0.11±0.03
	1 µM Can	0.07±0.02	0.09±0.03
	Aldo + Can	0.1±0.03	0.11±0.02

Table 1. Determination of ΔGSSP, ΔGSH in HC, PA and *in vitro* treated RBCs. Fresh blood was collected from HC and PA. For *in vitro* treatment, only blood from HC was utilized, and RBCs, were incubated at 37°C for 1h in absence (C) or presence of 2 or 5 nM aldosterone (Aldo) or 5 µM cortisol (Cort) or 1 µM canrenon (Can), alone or in association (Aldo+Cort or Aldo+Can), in charcoal-stripped plasma to remove small molecular weight macromolecules such as steroid and peptide hormones. After incubation, RBCs underwent hemolysis in hypotonic buffer.

ΔGSSP: Membranes, obtained from HC, PA and *In vitro* samples as described in Methods, were TCA-deproteinized and alkalinized, and the amount of GSH released from proteins was determined enzymatically in the supernatants, as described in Methods. The increase in glutathione released from RBCs membranes after diamide (1.5 mM) treatment, representing increase in glutathionylated protein content (ΔGSSP), is expressed as $\mathbf{(GSSP_{(D)}/GSSP_{(B)})-1}$.

ΔGSH: 10 µl of cytosol, obtained from HC, PA and *In vitro* samples as described in Methods, were analysed. Total glutathione was determined enzymatically and analysed spectrophotometrically at 412 nm. The total decrease in glutathione content after diamide treatment (ΔGSH) was expressed as $\mathbf{1-(GSH_{(D)}/GSH_{(B)})}$, being GSH_D glutathione content after diamide treatment and GSH_B that in untreated cells.

Being GSH only a part of the antioxidant defenses of the cell, cytosol was also investigate for CA activity and monomerization, both factors particularly sensitive to the oxidative state of the cell (Andrisani et al., 2014).

CA is a family of metallo-enzymes which catalyse the conversion of CO_2 to HCO_3^- and H^+, and is involved in many physiological processes such as acid–base balance homeostasis, respiration, carbon dioxide and ion transport, and bone resorption (Henry, 1996; Sly and Hu, 1995). This enzyme was also relevant for its sensitiveness to an increased oxidative status. In fact, when cytosol from untreated HC RBCs was analysed for CA detection by Western blotting (Fig. 12 A) and activity (Fig. 12 B) in the absence (lane a) or presence of 1.5 mM diamide for 10 (lane b) or 20 min (lane c), CA, present as dimer at 60 kDa, was shown to monomerize in time-dependent way and to increase its catalytic activity up to nine folds.

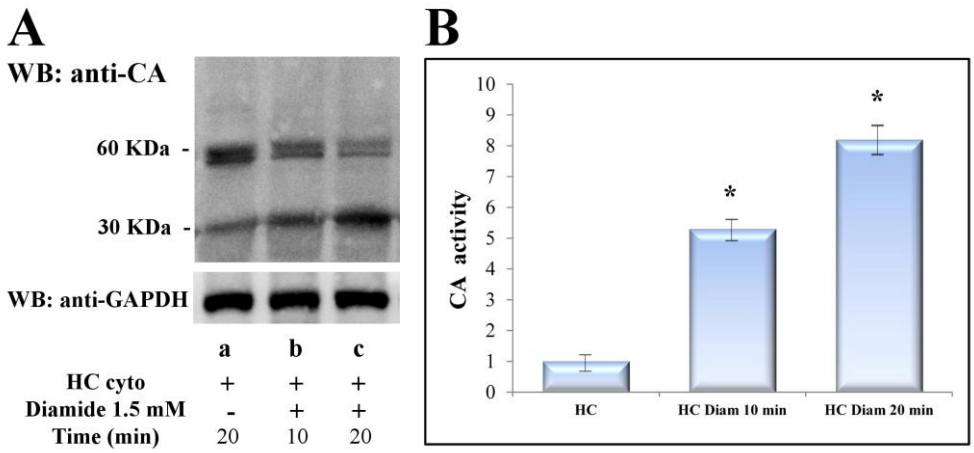

Figure 12. Panel A: Diamide-induced CA monomerization in HC RBCs cytosol. Fresh blood was collected from HC RBCs, isolated as described in Methods, and incubated with and without 1.5 mM diamide for 10 or 20 min. Diluted cytosol, obtained as described in Methods, underwent Western blotting in non-reducing conditions and was immunostained with anti-CA antibody.

Panel B: CA activity from 300 µl of diluted cytosol from HC RBCs incubated with and without 1.5 mM diamide for 10 or 20 min. CA activity calculated as ratio to activity observed in untreated cells (chosen as arbitrary comparison unit, experimentally determined as 1±0.21, mean value ± SD). Data show the means±SD of n=12 separate experiments.

* $p<0.0001$, comparison of CA activity, before and after diamide treatment, Student's t-test.

This was further confirmed in the previous study with endometriotic patients (EP) showing a net increase in CA activity compared to healthy controls (Andrisani et al., 2014). In this case, EP RBCs were also characterised by high degree of membrane glutathionylation and cytosolic GSH decrease, both parameters of a remarkable oxidative stress (Andrisani et al., 2014).

This analysis was extended to HC, PA and in vitro treated RBCs. No variation was found between HC and PA, nor in the differently *in vitro* treated HC RBCs (Table 2).

		Carbonic anhydrase		
	Samples	**Activity (mUnits /µl packed RBC)**	**30 KDa %**	**60 KDa %**
	HC	0.21±0.04	14±2	86±2
	PA	0.22±0.03	17±6	83±6
In vitro	**C**	0.19±0.06	15±3	85±3
	2 nM Aldo	0.20±0.05	16±2	84±2
	5 nM Aldo	0.18±0.05	18±4	82±4
	5 µM Cort	0.20±0.03	16±3	84±3
	Aldo + Cort	0.19±0.07	19±2	81±2
	1 µM Can	0.22±0.4	15±3	85±3
	Aldo + Can	0.17±0.07	13±3	87±3

Table 2. Determination of CA content and activity in HC, PA and *in vitro* treated RBCs. Fresh blood was collected from HC and PA. For *in vitro* treatment, only blood from HC was utilized, and RBCs, were incubated at 37°C for 1h in absence (C) or presence of 2 or 5 nM aldosterone (Aldo) or 5 µM cortisol (Cort) or 1 µM canrenone (Can), alone or in association (Aldo+Cort or Aldo+Can), in charcoal-stripped plasma to remove small molecular weight macromolecules such as steroid and peptide hormones. After incubation, RBCs underwent hemolysis in hypotonic buffer.

CA content in RBCs cytosol: Diluted cytosol from 1 µl of packed cells, obtained as described in Methods, underwent Western blotting in non-reducing conditions and was immunostained with anti-CA antibody. Densitometrical analysis of cytosol CA bands in HC, PA and *in vitro* samples RBCs was performed. Sum of 30 and 60 kDa bands arbitrarily calculated as 100%, taking into account that amount of proteolytic 30 kDa bands accounts for half the larger bands.

CA activity: 300 µl of diluted cytosol from RBCs of HC, PA and *in vitro* samples were analysed. The activity of carbonic anhydrase was assayed spectrophotometrically as

described in Methods. One unit of CA activity was defined as the amount of enzyme which catalyzes the formation of 1 pmol PNP/min in standard conditions of incubation. The mixture was incubated for 10 min at room temperature, and the following formula incorporating the extinction coefficient was used to calculate: CA Units $x10^{-3}$/ µl packed RBCs = OD × sample dilution factor /(min × 667), with an extinction coefficient of 667.
Values expressed as means±SD. Comparison HC vs PA and for in vitro experiments, C vs Aldo, Cort, Can, Aldo+Cort Aldo+Can. Student's t test reveals no statistical significance.

Taken together these data assess that PA RBCs seemed not to be subjected to increased oxidative stress, nor Aldo seemed to induce any alteration in the main parameters representative of the oxidative status, such as GSSG, GSSP, and CA.

3.2. Tyr-protein kinase and phosphatase assays

To further assess RBCs membrane status from both HC and PA patients and after *in vitro* treatments, Tyr-protein kinases and phosphatases distribution and activation were analysed. Previous studies demonstrated that diamide-induced Tyr-P of membrane band 3 involved the combined action of two different Tyr-kinases, Syk and Lyn, together with the counteracting activity of a Tyr-protein phosphatase, SHP2, responsible of the band 3 dephosphorylating process (Brunati et al., 2000; Bordin et al., 2002). Diamide, by oxidizing the catalytic cysteine residue of the Tyr-phosphatases, almost completely inhibited dephosphorylating process, thus evidencing phosphorylated residues. The differences showed in the band 3 Tyr-P level between HC and PA, as well as in the *in vitro* treatments, could be due to an imbalance between these two opposite activities.
Membranes, from HC, PA and *in vitro* treated RBCs were analysed by Western blotting and revealed with anti-Syk, anti-SHP-2 or anti-P-Src antibodies. Nor Syk or SHP-2 resulted differently recruited to membranes (data not shown), indicating no constitutive alteration of the different membranes. Interestingly, anti-P-Src evidenced a net increase of the phosphorylated activated isoform of the Src family members in the PA group compared to HC (145±5% compared to 100±3%), and further confirmed in the in vitro experiments by Aldo addition (Table 3).

	Samples	pSrc (%)	PTK Activity (%)	PTP Activity (%)
	HC	100±3	100±2	100±4
	PA	145±5 *	115±3 *	103±5
In vitro	**C**	102±2	101±3	101±3
	2 nM Aldo	134±4 *	108±5 *	104±3
	5 nM Aldo	167±4 *	126±4 *	105±4
	5 µM Cort	104±3	103±2	104±4
	Aldo + Cort	109±5	107±4	103±2
	1 µM Can	101±3	101±3	99±5
	Aldo + Can	103±2	103±4	101±3

Table 3. P-Src contents, protein tyrosin kinases (PTK) and protein tyrosin phosphatases (PTP) activity in HC, PA or *in vitro* treated RBCs. Fresh blood was collected from HC and PA and RBCs were isolated as described in Methods. For *in vitro* treatment, only blood from HC was utilized, and RBCs, were incubated at 37°C for 24 h in absence (C) or presence of 2 or 5 nM aldosterone (Aldo) or 5 µM cortisol (Cort) or 1 µM canrenone (Can), alone or in association (Aldo+Cort or Aldo+Can), in charcoal-stripped plasma to remove small molecular weight macromolecules such as steroid and peptide hormones. After incubation, RBCs underwent hemolysis in hypotonic buffer.

P-Src content: RBCs membranes underwent Western blotting and were revealed with anti-P-Src or anti-actin antibody as loading control. Bands were scanned densitometrically. The values were obtained as the ratio percentage to the P-Src content of RBCs from HCs (chosen as arbitrary comparison units). The figure is representative of 12 separate experiments.

PTK and PTP activity: membranes were analyzed for PTK and PTP activity as described in Methods. The values were obtained as the ratio percentage to PTK or PTP activity of RBCs from HCs (chosen as arbitrary comparison units). The figure is representative of 12 separate experiments.

* $p<0.001$, comparison of p-Src, PTK or PTP % of HC *vs* PA; for *in vitro* experiments comparison of C *vs* all other samples; Student's t-test.

When both Tyr-kinase and phosphatase assays were performed in membranes from RBC incubated in the absence of diamide, a 15% increase of the Tyr-kinase activity, but not of the Tyr-phosphatase counterpart, was substantiated in PA group, reaching the 25% in Aldo-treated RBCs (Table 3). When the same assay was performed in membrane from diamide-treated RBCs, PTK resulted similar if

not identical to that of diamide-untreated RBC (not shown), whereas PTPase activity was almost completely inhibited by diamide, as expected (not showon).
This slight increase of the Tyr-kinase activity, however, was not sufficient to induce a net imbalance in the Tyr-phosphorylation process of membranes from RBCs not incubated with diamide, as indicated by the absence of phosphorylation in both PA and Aldo-treated RBCs, which remained similar to HC RBCs.

3.3. Evaluation of the redox-related band 3 aggregates formation

To evidence if membrane band 3 aggregation was under redox regulation, we subjected membranes to Western blotting in both non reducing and reducing conditions. Results showed that membranes from HC RBC incubated with Aldo increasing concentrations contained increasing band 3 aggregates (Fig. 13) which were promptly and completely reversed in the presence of β-mercaptoethanol, the reducing effector.

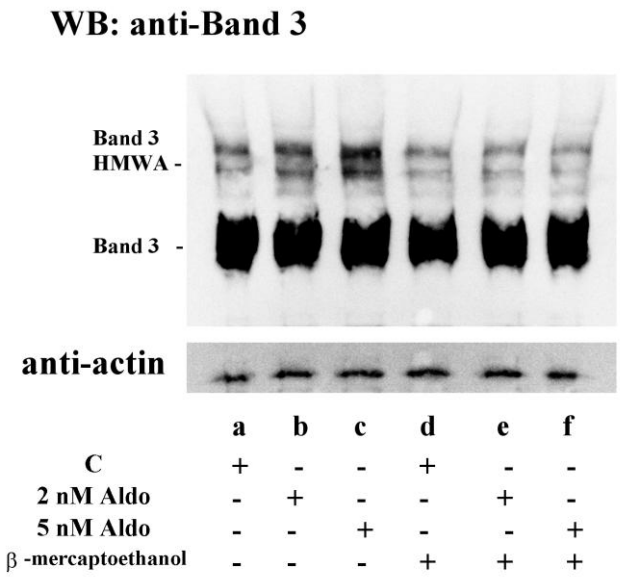

Figure 13. Band 3 HMWA contents *in vitro* treated RBCs. HC RBCs, isolated as described in Methods, were incubated at 37°C for 24 h in absence (C) or presence of 2 or 5 nM aldosterone (Aldo) in charcoal-stripped plasma. After incubation, RBCs underwent hemolysis in hypotonic buffer. RBCs membranes underwent Western blotting in non-reducing conditions (lane a, b and c) or in reducing conditions (addition of β-

mercaptoethanol; lane d, e and f) and were revealed with anti-band 3 or anti-actin antibody as loading control. The figure is representative of 12 separate experiments.

Similar results were also obtained when PA RBC membranes were analyzed, and the comparison among the different conditions were reported in Table 4.

		Band 3 HMWA	
	Samples	**NR**	**R**
	HC	1.00±0.04	1.00±0.02
	PA	1.97±0.12 *	1.02±0.06
In vitro	**C**	1.02±0.03	0.99±0.04
In vitro	**2 nM Aldo**	1.32±0.19 *	1.04±0.03
In vitro	**5 nM Aldo**	1.78±0.15 *	0.98±0.05

Table 4. Band 3 HMWA contents in HC, PA or *in vitro* treated RBCs. Fresh blood was collected from HC and PA and RBCs were isolated as described in Methods. For *in vitro* treatment, only blood from HC was utilized, and RBCs, were incubated at 37°C for 24 h in absence (C) or presence of 2 or 5 nM aldosterone (Aldo) in charcoal-stripped plasma. After incubation, RBCs underwent hemolysis in hypotonic buffer. RBCs membranes underwent Western blotting in non-reducing conditions (NR) or in reducing conditions (R) and were revealed with anti-band 3 or anti-actin antibody as loading control. Bands were scanned densitometrically. Band 3 HMWA values were obtained as the ratio to the HMWA content of RBCs from HCs (chosen as arbitrary comparison units), respectively, in non-reducing or reducing conditions. The figure is representative of 12 separate experiments.

* $p<0.001$, comparison of band 3 HMWA of HC *vs* PA and, for *in vitro* experiments, comparison of C *vs* all other samples, respectively in non-reducing or reducing conditions, Student's t-test.

DISCUSSION

MR activity has long been related to the genomic response occurring after half/an hour from Aldo addition and involving Aldo-MR shifting to the nucleus to regulate gene transcription. Recently, growing evidences of an early non-genomic response have been related to direct Aldo effects on protein kinases, Na+/H+ exchangers and NADPH oxidase (Dooley et al., 2012; Hayashi et al., 2008). In fact, beside the essential role of Aldo in regulating hydro/saline homeostasis, recent studies have emphasized its involvement in the occurrence of inflammatory status, both local (Hayashi et al., 2008) and general (Calò et al., 2004). Aldo promotes tissue inflammation, leading to fibrosis and tissue remodeling in the heart, vascular system, and kidney (Shibata and Fujita, 2012; Egido, 1996; Berl et al., 1978). It also contributes to generalized inflammatory status by activating circulating mononuclear cells, as shown by the Aldo-induced expression of PAI1 and p22phox (Calò et al., 2004) and, non-genomically, by directly activating NADPH-oxidase dependent oxidative species production (Hayashi et al., 2008).

We demonstrated that RBCs from PA patients display as similar membrane alterations to those previously observed in other inflammation diseases, such as endometriosis and PCOs (Bordin et al., 2010b; Donà et al., 2012), two clinical situations where Aldo or Aldo/PRA ratio are higher than in controls. These alterations can be observed in the presence of an adjunctive stress, such as that induced by diamide, which can trigger band 3 Tyr-P to a remarkably higher level in patients, as compared to HCs (Fig. 1). This could be due to an unbalance of the antithetic activities of Tyr-protein kinases and phosphatases, or to membrane reorganization, exposing band 3 target differently to the above activities. The higher HMWA content found in PA RBCs (Fig. 2) indicates a sensible alteration of the target band 3 and, hence, of the membranes, since band 3, as integral protein, is responsible for the interaction between the bilayer and the underlying cytoskeleton.

Similar results were obtained in vitro by incubating CS-PPP RBCs from HCs in the presence of Aldo, showing that a non-genomic effect of Aldo in RBCs is mediated by the classic MR, which was evidenced in RBCs cytosol. MR involvement in the Aldo-related signaling was further confirmed by the findings that both Can and Cort prevented Aldo-induced alterations.

Moreover Aldo dose and time dependently increases band 3 HMWA formation and augments RBCs IgG binding, consistent with an involvement of Aldo in premature RBC aging. To date and to our knowledge, no evidence has been reported about a clear antagonistic effect of Cort in the non-genomic signaling of Aldo-MR. (Published in : Bordin et al., 2013)

Further investigations regarding the possible role of Cort in RBCs from patients with PA also would be helpful in the comprehension of steroid hormone signaling.

To completion of the previous study, we demonstrated the presence of MR in the RBC cytosol (Fig. 6), thus giving a clear explanation to the antagonistic/blocking effects of Cort or Can co-incubation with Aldo in *in vitro* experiments. To investigate the effective pathway involved, we further investigated cytosol where we found that, in non-activated conditions, such as in the absence of Aldo and other steroid hormones (CS-PPP), MR is mainly complexed in a multiprotein aggregate, which ensures it has the correct conformation for binding effectors. When Aldo is added, it binds to MR, causes it to break away from the complex, as shown by the shifting of the molecular weight of MR in the glycerol gradient, and induces it to form dimers (Fig. 7). Aldo-MR dimers have a short life-span, as shown by the time-dependent increase of MR destruction in low molecular weight fragments (Figs. 7 and 8) thus ensuring signal shutdown and sequestration of Aldo in the proteolysed fragments (data not shown), in a sort of Aldo scavenging from circulation.

Concomitantly, in the membranes, Aldo induced alterations were mainly detectable after 24 h of incubation in a dose- and time-dependent manner (Figs. 4

and 5), and consisted of band 3 aggregation and circulating IgG binding (Bordin et al., 2013).

When Aldo is replaced by Cort, MR shifted slightly from the gradient area of the MR complex in the early 30 min of incubation (data not shown), after which MR reconstituted its initial complex (Fig. 7). This is in line with the fact that Cort did not induce alterations in RBC membranes but, when added with Aldo, prevented Aldo-mediated alterations (Bordin et al., 2013).

Can did not cause any alteration in the complex, but completely avoided Aldo-induced disaggregation and alterations in membranes (Bordin et al., 2013).

Interestingly, in both Aldo-MR dimer and MR-complex, MR binding is regulated by redox conditions, as shown by the differences in reducing and non-reducing conditions (compare Figs. 7 and 8). In addition, the observation that the anti-MR antibody used for the immunoprecipitation, recognizing the N-terminal region (aa. 1-300) of the MR, did not bind to MR when dimerised or complexed, suggests that this region is involved in dimer/complex formation (Fig. 9). This was further confirmed by Cort inducing MR release but not dimerization. In this way, the N-terminal region of Cort-MR remains free: a) to be recognized by the antibody; b) to re-associate with the multi-protein complex, by releasing Cort, thus maintaining the correct conformation for potential later Aldo binding. In addition, MR re-association prevents MR degradation, which was only slightly higher than in controls, thus contributing to MR reserve maintenance.

As determinant part of the complex, the chaperone protein HSP90 has a central role in the MR activation. Gelda, which binds to the N-terminal domain ATP binding site of HSP90 and inhibits the chaperone activity of the HSP90 (Stebbins et al., 1997), succeeded in releasing MR from the complex completely but prevented Aldo-induced MR dimerization, thus confirming that the multi-protein complex is fundamental in maintaining MR in the correct conformation for later Aldo binding. This was further demonstrated by the fact that when HC RBCs were pre-incubation with Gelda, Aldo failed to evoke membrane alterations leading to IgG binding (Fig. 10), thus confirming that intact complex is needed for the correct Aldo MR response.

HSP90 is known to be involved in cell proteostasis by chaperoning native proteins into multiprotein complex to prevent misfolding and turn over. HSP90 associates with a number of signaling proteins (Mjahed et al., 2012) ensuring their stability and correct functioning in the regulation of the programmed cell death. The involvement of cytosolic HSP90-multiprotein complex in the development of cell patho-physiology has been recently assessed in B-cell chronic lymphocytic leukemia where HSP90 association with Lyn's dysregulated expression, activity, and localization supported abnormal cell survival by inhibiting an early player of apoptotic signaling. (Contri et al., 2005; Zonta et al., 2014).

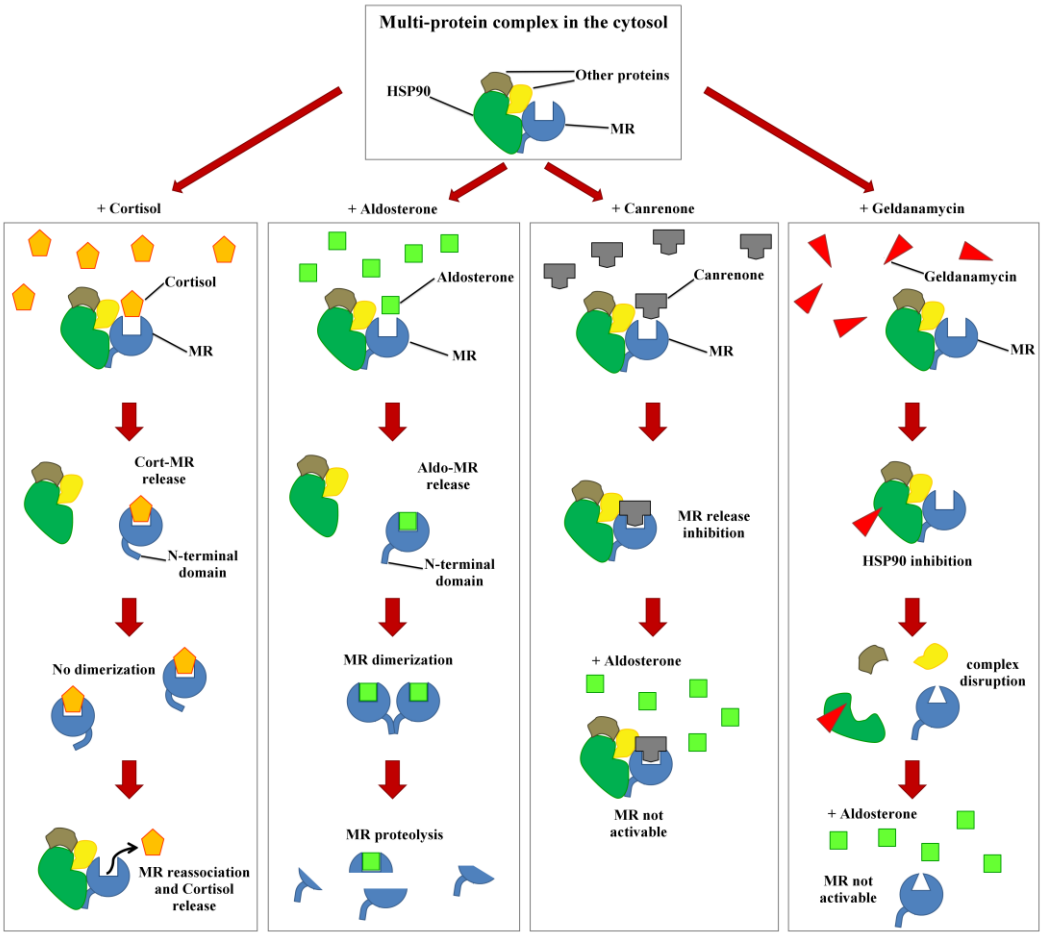

Figure 14. MR regulation by Cort, Aldo, Can and HSP90 inhibitor.

In conclusion, our data demonstrate that in human RBCs a genomic-like Aldo signaling involves MR activation, dimerization and proteolysis but avoids gene transcription and oxidative intermediates. This MR-mediated response involves

ligand specificity, with Aldo inducing MR activation leading to RBCs membrane alterations and IgG binding (Bordin et al., 2013) and Cort preventing MR activation. This different ligand-dependent recruitment of MR has not yet been demonstrated in other tissues where MR specificity for Aldo was tightly related to the expression of 11-beta-hydroxysteroid dehydrogenase 2, which transforms Cort to cortisone thus preventing MR inappropriate activation (Albiston et al., 1994). The evidence that Aldo-induced activation/dimerization is regulated by oxide-reductive conditions and HSP90-chaperoned complex integrity may be also useful for the better comprehension of potential complications in PA.

At last, due to the reported pro-oxidative effect of Aldo (Pu et al., 2003; Kotlyar et al., 2006; Patni et al., 2007; Yamaji et al., 2009; Calò et al., 2010; Stehr et al., 2010), our investigations focuses on potential traces of oxidative intermediates generated by the Aldo-induced MR activation and acting at membrane level.
The redox state of the cell was evaluated by assessing the contents of both cytosolic ΔGSH and that of glutathionylated proteins (GSSP) in the absence or presence of diamide. In facts, as previously shown in other inflammatory diseases, diamide treatment enhances eventual pre-existent alterations of the cell membrane proteins, by inducing disulfide bond formations between GSH and the SH group of protein cysteine residues to form GS-SP. When GSH content was tested in cytosol or membranes from RBC previously incubated in the absence or presence of diamide, the addition of glutathione reductase, which should reduce disulfide and reconstituted the initial condition in the same extent in patients and in controls.

The difference between the GSH content without and with diamide may be directly related to the oxidative state of membrane proteins (Bordin et al., 2010b).
Neither GSSG nor GSSP were altered in either PA patients or in *in vitro* experiments with increasing concentrations of Aldo (Table 1), thus excluding an oxidative process involving glutathione-mediated processes in the Aldo-related alterations.

However, cells contain complex systems of multiple types of antioxidants, such as vitamins as well as enzymes such as catalase, superoxide dismutase and various peroxidases, all able to counteract specifically different forms of oxidative assault. To obviate the need to test each of the above anti-oxidants, we monitored a cytosolic protein, CA, which we demonstrated to be particularly sensitive to high oxidative status. In fact, we demonstrated that this enzyme, generally present in dimeric 60 kDa isomer, is particularly sensitive to oxidative-related transformation, yielding a 30 kDa isomer which is much more active than the larger one. CA activity is mainly and directly related to the amount of 30 kDa monomer available in the cellular compartment, as also demonstrated by diamide-induced monomerization and activation (Fig. 12). CA activity and monomerization showed no differences between HC and PA groups, nor any alteration was detectable in *in vitro* experiments with increasing Aldo concentrations (Table 2), thus further confirming that Aldo did not induce membrane alterations through a common oxidative-related way, but through a different signaling pathway.

To better understand membrane alterations inducing band 3 aggregation, we compared membranes in both reducing and non-reducing conditions. Whereas in non-reducing conditions band 3 aggregated mostly in PA RBCs as well as in Aldo treated cells, as previously demonstrated (part 1; Bordin et al., 2013), in reducing conditions band 3 HMWA content was almost completely identical both comparing HC and PA groups, and HC RBCs incubated in the presence of increasing Aldo concentrations. That no difference was detectable in membranes of patients or after Aldo treatment suggests that band 3 aggregation was dependent on the oxidation of SH-groups, since β-mercaptoethanol, reducing effector used to induce reducing conditions, affects principally protein disulfide bonds. That this clusterization may be due to an oxidative process or membrane alterations, leading to band 3 aggregation, was at the basis of a successive cysteine auto-oxidation was not investigated and would be further addressed in forthcoming studies. Anyway, in the first case, it should be ruled out that Aldo-MR signaling involves a “mediator”, able to oxidize band 3 cysteines, whereas, in

the second case, it triggers a “mediator” able to induce such membrane alterations that band 3 clusters thus leading to successive auto-oxidation. The common factor remains Aldo-MR activation as further demonstrated by the successive results. In facts, in *in vitro* experiments, when Aldo was added in association with Gelda, an inhibitor of the HSP90 protein, neither HMWA nor IgG binding was observed, thus confirming once more that Aldo effects were mediated by the activation of the cytosolic MR, which needs the association in the HSP90 multiprotein complex to be kept in the correct conformation for the eventual activation.

In conclusion, we found that in PA RBCs Aldo is responsible for the membrane alterations leading to a potential premature removal of the cells from circulation. Aldo exerts its effect through the activation of the soluble MR complex, which participates in the modulation of the Aldo signaling through the possibility of being differently affected by other steroids or Aldo inhibitors (Can). In addition, membrane alterations are related to band 3 aggregation through disulfide bond formation, though no common parameter of oxidative assault was evidenced.
Further studies are in progress to explore both nature and potential mediators of the Aldo-induced alterations in the band 3 dimer formation.

REFERENCES

Albiston AL, Obeyesekere VR, Smith RE, Krozowski ZS. (1994) Cloning and tissue distribution of the human 11 beta-hydroxysteroid dehydrogenase type 2 enzyme. *Mol Cell Endocrinol* 105: R11–R17.

Andrisani A, Donà G, Brunati AM, Clari G, Armanini D, Ragazzi E, Ambrosini G, Bordin L. (2014) Increased oxidation-related glutathionylation and carbonic anhydrase activity in endometriosis. *Reprod Biomed Online* 28: 773-779.

Arese P, Turrini F, Schwarzer E. (2005) Band 3/complement-mediated recognition and removal of normally senescent and pathological human erythrocytes. *Cell Physiol Biochem* 16(4-6): 133-146.

Baker ME, Funder JW, Kattoula SR. (2013) Evolution of hormone selectivity in glucocorticoid and mineralocorticoid receptors. *J Steroid Biochem Mol Biol* 137: 57–70.

Bellelli A, Brunori M. (2011) Hemoglobin allostery: variations on the theme. *Biochim Biophys Acta* 1807(10): 1262-1272.

Berl T, Katz F H, Henrich W L, de Torrente A, Schrier RW. (1978) Role of aldosterone in the control of sodium excretion in patients with advanced chronic renal failure. *Kidney Int* 14: 228–235.

Boldyreff B, Wehling M. (2003) Non-genomic actions of aldosterone: mechanisms and consequences in kidney cells. *Nephrol Dial Transplant* 18: 1693-1695.

Bordin L, Brunati AM, Donella-Deana A, Baggio B, Toninello A, Clari G. (2002) Band 3 is an anchor protein and a target for SHP-2 tyrosine phosphatase in human erythrocytes. *Blood* 100(1): 276-82.

Bordin L, Fiore C, Zen F, Coleman MD, Ragazzi E, Clari G. (2010a) Dapsone hydroxylamine induces premature removal of human erythrocytes by membrane reorganization and antibody binding. *Br J Pharmacol* 161: 1186-1199.

Bordin L, Fiore C, Donà G, Andrisani A, Ambrosini G, Faggian D, Plebani M, Clari G, Armanini D. (2010b) Evaluation of erythrocyte band 3 phosphotyrosine level,

glutathione content, CA-125, and human epididymal secretory protein E4 as combined parameters in endometriosis. *Fertil Steril* 94: 1616-1621.

Bordin L, Ion-Popa F, Brunati AM, Clari G, Low PS. (2005a) Effector-induced Syk-mediated phosphorylation in human erythrocytes. *Biochim Biophys Acta* 1745: 20-28.

Bordin L, Zen F, Ion-Popa F, Barbetta M, Baggio B, Clari G. (2005b) Band 3 Tyr-phosphorylation in normal and glucose-6-phosphate dehydrogenase-deficient human erythrocytes. *Mol Membr Biol* 22: 411-420.

Bordin L, Quartesan S, Zen F, Vianello F, Clari G. (2006) Band 3 Tyr-phosphorylation in human erythrocytes from non-pregnant and pregnant women. *Biochim Biophys Acta* 1758: 611-619.

Bordin L, Donà G, Sabbadin C, Ragazzi E, Andrisani A, Ambrosini G, Brunati AM, Clari G, Armanini D. (2013) Human red blood cells alterations in primary aldosteronism. *J Clin Endocrinol Metab* 98: 2494-2501.

Bordin L, Clari G, Moro I, Dalla Vecchia F, Moret V. (1995) Functional link between phosphorylation state of membrane proteins and morphological changes of human erythrocytes. *Biochem Biophys Res Commun* 213: 249-257.

Bosman GJ, Lasonder E, Groenen-Döpp YA, Willekens FL, Werre JM, Novotný VM. (2010) Comparative proteomics of erythrocyte aging in vivo and in vitro. *J Proteomics* 73: 396-402.

Bosman GJ, Willekens FL, Werre JM. (2005) Erythrocyte aging: a more than superficial resemblance to apoptosis? *Cell Physiol Biochem* 16: 1-8.

Bratosin D, Mazurier J, Tissier JP, Estaquier J, Huart JJ, Ameisen JC, Aminoff D, Montreuil J. (1998) Cellular and molecular mechanisms of senescent erythrocyte phagocytosis by macrophages. A review. *Biochimie* 80: 173-195.

Brautigan DL. (1992) Great expectation: protein tyrosine phosphatase in cell regulation. *Biochim Biophys Acta* 1114: 63-77.

Briet M, Schiffrin EL. (2011) The role of aldosterone in the metabolic syndrome. *Curr Hypertens Rep* 13(2): 163-172.

Brown MT, Cooper JA. (1996) Regulation, substrates and functions of src. *Biochim Biophys Acta* 1287: 121-149.

Brunati AM, Bordin L, Clari G, James P, Quadroni M, Baritono E, Pinna LA, Donella-Deana A. (2000) Sequential phosphorylation of protein band 3 by Syk and Lyn tyrosine kinases in intact human erythrocytes. Identification of primary and secondary phosphorylation sites. *Blood* 96: 1550-1557.

Brunati AM, Bordin L, Clari G, Moret V. (1996) The Lyn catalyzed Tyr phosphorylation of the transmembrane band 3 protein of human erythrocytes. *Eur J Biochem* 240: 394-399.

Calò LA, Pagnin E, Davis PA, Armanini D, Mormino P, Rossi GP, Pessina AC. (2010) Oxidative stress-related proteins in a Conn's adenoma tissue. Relevance for aldosterone's prooxidative and proinflammatory activity. *J Endocrinol Invest* 33: 48-53.

Calò LA, Zaghetto F, Pagnin E, Davis PA, De Mozzi P, Sartorato 1 P, Martire G, Fiore C, Armanini D. (2004) Effect of aldosterone and glycyrrhetinic acid on the protein expression of PAI-1 and p22(phox) in human mononuclear leukocytes. *J Clin Endocrinol Metab* 89: 1973-1976.

Connell JM and Davies E. (2005) The new biology of aldosterone. *J Endocrinol* 186(1): 1-20.

Contri A, Brunati AM, Trentin L, Cabrelle A, Miorin M, Cesaro L, Pinna LA, Zambello R, Semenzato G, Donella-Deana A. (2005) Chronic lymphocytic leukemia B cells contain anomalous Lyn tyrosine kinase, a putative contribution to defective apoptosis. *J Clin Invest* 115: 369-378.

De Franceschi L, Fumagalli L, Olivieri O, Corrocher R, Lowell CA, Berton G. (1997) Deficiency of Src family kinases Fgr and Hck results in activation of erythrocyte K/Cl cotransport. *J Clin Invest* 99: 220-227.

De Neef RS, Hardy-Dessources MD, Giraud F. (1996) Relationship between type II phosphatidylinositol 4-kinase activity and protein tyrosine phosphorylation in membranes from normal and sickle red cells. *Eur J Biochem* 235: 549-556.

Di Simplicio P, Cacace MG, Lusini L, Giannerini F, Giustarini D, Rossi R. (1998) Role of protein -SH groups in redox homeostasis – the erythrocyte as a model system. *Arch Biochem Biophys* 355: 145–152.

Donà G, Sabbadin C, Fiore C, Bragadin M, Giorgino FL, Ragazzi E, Clari G, Bordin L, Armanini D. (2012) Inositol administration reduces oxidative stress in

erythrocytes of patients with polycystic ovary syndrome. *Eur J Endocrinol* 166: 703-710.

Donella-Deana A, Cesaro L, Ruzzene M, Brunati AM, Marin O, Pinna LA. (1998) Spontaneous autophosphorylation of Lyn tyrosine kinase at both its activation segment and C-terminal tail confers altered substrate specificity. *Biochemistry* 37: 1438-1446.

Dooley R, Harvey BJ, Thomas W. (2012) Non-genomic actions of aldosterone: from receptors and signals to membrane targets. *Mol Cell Endocrinol* 350: 223-234.

Egido J. (1996) Vasoactive hormones and renal sclerosis. *Kidney Int* 49: 578–597.

Faresse N. (2014) Post-translational modifications of the mineralocorticoid receptor: How to dress the receptor according to the circumstances? *J Steroid Biochem Mol Biol* 143: 334–342.

Ferru E, Giger K, Pantaleo A, Campanella E, Grey J, Ritchie K, Vono R, Turrini F, Low PS. (2011) Regulation of membrane-cytoskeletal interactions by tyrosine phosphorylation of erythrocyte band 3. *Blood* 117: 5998-6006.

Fuller PJ, Lim-Tio SS, Brennan FE. (2000) Specificity in mineralocorticoid versus glucocorticoid action. *Kidney Int* 57: 1256–1264.

Funder JW. (2010) Aldosterone, hypertension and heart failure: insights from clinical trials. *Hypertens Res* 33: 872-875.

Funder JW. (2011) Medicine. The genetics of primary aldosteronism. *Science* 331: 685-686.

Geers C, Gros G. (2000) Carbon dioxide transport and carbonic anhydrase in blood and muscle. *Physiol Rev* 80(2): 681-715.

Gilmour KM. (2010) Perspectives on carbonic anhydrase. *Comp Biochem Physiol A Mol Integr Physiol* 157(3): 193-197.

Grek CL, Zhang J, Manevich Y, Townsend DM, Tew KD. (2013) Causes and consequences of cysteine S-glutathionylation. *J Biol Chem* 288(37): 26497-26504.

Grossmann C, Gekle M. (2009) New aspects of rapid aldosterone signaling. *Mol Cell Endocrinol* 30: 853–862.

Harrison ML, Isaacson CC, Burg DL, Geahlen RL, Low PS. (1994) Phosphorylation of human erythrocyte band 3 by endogenous p72syk. *J Biol Chem* 269: 955-959.

Harrison ML, Rathinavelu P, Arese P, Geahlen RL, Low PS. (1991) Role of band 3 tyrosine phosphorylation in the regulation of erythrocyte glycolysis. *J Biol Chem* 266: 4106-4111.

Hattangady NG, Olala LO, Bollag WB, Rainey WE. (2012) Acute and chronic regulation of aldosterone production. *Mol Cell Endocrinol* 350(2): 151-162.

Hayashi H, Kobara M, Abe M, Tanaka N, Gouda E, Toba H, Yamada H, Tatsumi T, Nakata T, Matsubara H. (2008) Aldosterone nongenomically produces NADPH oxidase-dependent reactive oxygen species and induces myocyte apoptosis. *Hypertens Res* 31: 363-375.

Henry RP. (1996) Multiple roles of carbonic anhydrase in cellular transport and metabolism. *Annu Rev Physiol* 58: 523-538.

Herzberg V, Boughter JM, Carlisle S, Hill DE. (1980) Evidence for two insulin receptor populations on human erythrocytes. *Nature* 286: 279-281.

Jay DG. (1996) Role of band 3 in homeostasis and cell shape. *Cell* 86: 853–854.

Jennings ML. (1985) Kinetics and mechanism of anion transport in red blood cells. *Annu Rev Physiol* 47: 519-533.

Keidar S, Gamliel-Lazarovich A, Kaplan M, Pavlotzky E, Hamoud S, Hayek T, Karry R, Abassi Z. (2005) Mineralocorticoid receptor blocker increases angiotensin-converting enzyme 2 activity in congestive heart failure patients. *Circ Res* 97: 946-953.

Kotlyar E, Vita JA, Winter MR, Awtry EH, Siwik DA, Keaney Jr JF, Sawyer DB, Cupples LA, Colucci WS, Sam F. (2006) The relationship between aldosterone, oxidative stress, and inflammation in chronic, stable human heart failure. *J Cardiac Fail* 12: 122-127.

Koury MJ. (2014) Abnormal erythropoiesis and the pathophysiology of chronic anemia. *Blood Rev* 28(2):49-66.

Laffer CL, Bolterman RJ, Romero JC, Elijovich F. (2006) Effect of salt on isoprostanes in salt-sensitive essential hypertension. *Hypertension* 47: 434-440.

Lang F, Qadri SM. (2012) Mechanisms and significance of eryptosis, the suicidal death of erythrocytes. *Blood Purif* 33: 125-130.

Lastra G, Dhuper S, Johnson MS, Sowers JR. (2010) Salt, aldosterone, and insulin resistance: impact on the cardiovascular system. *Nat Rev Cardiol* 7(10): 577-584.

Lenzini L, Rossi GP. (2014) The molecular basis of primary aldosteronism: from chimeric gene to channelopathy. *Curr Opin Pharmacol* 21C: 35-42.

Lother A, Moser M, Bode C, Feldman RD, Hein L. (2015) Mineralocorticoids in the heart and vasculature: new insights for old hormones. *Annu Rev Pharmacol Toxicol* 55: 289-312.

Low PS. (1986) Structure and function of the cytoplasmic domain of band 3: center of erythrocyte membrane-peripheral protein interactions. *Biochim Biophys Acta* 864: 145-167.

Low PS, Rathinavelu P, Harrison ML. (1993) Regulation of glycolysis via reversible enzyme binding to the membrane protein band 3. *J Biol Chem* 268: 14627-14631.

Luna EJ, Hitt AL. (1992) Cytoskeleton-plasma membrane interactions. *Science* 258(5084): 955-964.

Lutz HU, Fasler S, Stammler P, Bussolino F, Arese P. (1988) Naturally occurring anti-band 3 antibodies and complement in phagocytosis of oxidatively-stressed and in clearance of senescent red cells. *Blood Cells* 14: 175-203.

Marengo-Rowe AJ. (2006) Structure-function relations of human hemoglobins. *Proc (Bayl Univ Med Cent)* 19(3): 239-245.

Minetti G, Seppi C, Ciana A, Balduini C, Low PS, Brovelli A. (1998) Characterization of the hypertonically induced tyrosine phosphorylation of erythrocyte band 3. *Biochem J* 335: 305-311.

Mjahed H, Girodon F, Fontenay M, Garrido C. (2012) Heat shock proteins in hematopoietic malignancies. *Exp Cell Res* 318: 1946-1958.

Mohandas N, Gallagher PG. (2008) Red cell membrane: past, present, and future. *Blood* 112(10): 3939-3948.

Musch MW, Hubert EM, Goldstein L. (1999) Volume expansion stimulates p72syk and p56lyn in skate erythrocytes. *J Biol Chem* 274: 7923-7928.

Nakamura T, Kataoka K, Fukuda M, Nako H, Tokutomi Y, Dong YF, Ichijo H, Ogawa H, Kim-Mitsuyama S. (2009) Critical role of apoptosis signal-regulating

kinase 1 in aldosterone/salt-induced cardiac inflammation and fibrosis. *Hypertension* 54: 544-551.

Pacifici RE, Davies KJ. (1990) Protein degradation as an index of oxidative stress. *Methods Enzymol* 186: 485-502.

Pantaleo A, Giribaldi G, Mannu F, Arese P, Turrini F. (2008) Naturally occurring anti-band 3 antibodies and red blood cell removal under physiological and pathological conditions. *Autoimmun Rev* 7(6): 457-462.

Patni H, Mathew JT, Luan L, Franki N, Chander PN, Singhal PC. (2007) Aldosterone promotes proximal tubular cell apoptosis: role of oxidative stress. *Am J Physiol Renal Physiol* 293: 1065-1071.

Pu Q, Neves MF, Virdis A, Touyz RM, Schiffrin EL. (2003) Endothelin antagonism on aldosterone-induced oxidative stress and vascular remodeling. *Hypertension* 42: 49-55.

Qin W, Rudolph A, Bond BR, Rocha R, Blomme EA, Goeliner JJ, Funder JW, McMahon EG. (2003) Transgenic model of aldosterone-driven cardiac hypertrophy and heart failure. *Circ Res* 93: 69-76.

Reil JC, Hohl M, Selejan S, Lipp P, Drautz F, Kazakow A, Münz BM, Müller P, Steendijk P, Reil GH, Allessie MA, Böhm M, Neuberger HR. (2012) Aldosterone promotes atrial fibrillation. *Eur Heart J* 33: 2098-2108.

Robert-Nicoud M, Flahaut M, Elalouf JM, Nicod M, Salinas M, Bens M, Doucet A, Wincker P, Artiguenave F, Horisberger JD, Vandewalle A, Rossier BC, Firsov D. (2001) Transcriptome of a mouse kidney cortical collecting duct cell line: effects of aldosterone and vasopressin. *Proc Natl Acad Sci U.S.A.* 98: 2712-2716.

Rocha R, Chander PN, Khanna K, Zuckerman A, Stier CT Jr. (1998) Mineralocorticoid blockade reduces vascular injury in stroke-prone hypertensive rats. *Hypertension* 31: 451-458.

Salomao M, Zhang X, Yang Y, Lee S, Hartwig JH, Chasis JA, Mohandas N, An X. (2008) Protein 4.1R-dependent multiprotein complex: new insights into the structural organization of the red blood cell membrane. *Proc Natl Acad Sci USA* 105(23): 8026-8031.

Shibata S, Fujita T. (2012) Mineralocorticoid receptors in the pathophysiology of chronic kidney diseases and the metabolic syndrome. *Mol Cell Endocrinol* 350: 273-280.

Sly WS, Hu PY. (1995) Human carbonic anhydrases and carbonic anhydrase deficiencies. *Annu Rev Biochem* 64: 375-401.

Smith JE. (1987) Erythrocyte membrane: structure, function, and pathophysiology. *Vet Pathol* 24(6): 471-476.

Spat A, Hunyady L. (2004) Control of aldosterone secretion: a model for convergence in cellular signaling pathways. *Physiol Rev* 84: 489–539.

Stadtman ER, Levine RL. (2000) Protein oxidation. *Ann NY Acad Sci* 899: 191-208.

Stebbins CE, Russo AA, Schneider C, Rosen N, Hartl FU, Pavletich NP. (1997) Crystal structure of an Hsp90-geldanamycin complex: targeting of a protein chaperone by an antitumor agent. *Cell* 89: 239-250.

Stehr CB, Mellado R, Ocaranza MP, Carvajal CA, Mosso L, Becerra E, Solis M, Garcia L, Lavandero S, Jalil J, Fardella CE. (2010) Increased levels of oxidative stress, subclinical inflammation, and myocardial fibrosis markers in primary aldosteronism patients. *J Hypertens* 28: 2120-2126.

Swynghedauw B. (1999) Molecular mechanisms of myocardial remodeling. *Physiol Rev* 79: 215-262.

Tanner MJ. (2002) Band 3 anion exchanger and its involvement in erythrocyte and kidney disorders. *Curr Opin Hematol* 9(2): 133–139.

Tibaldi E, Brunati AM, Massimino ML, Stringaro A, Colone M, Agostinelli E, Arancia G, Toninello A. (2008) Src-Tyrosine kinases are major agents in mitochondrial tyrosine phosphorylation. *J Cell Biochem* 104(3): 840-849.

Tietze F. (1969) Enzymic method for quantitative determination of nanogram amounts of total and oxidized glutathione: applications to mammalian blood and other tissues. *Anal Biochem* 27: 502–522.

Tylicki L, Rutkowski P, Renke M, Larczynski W, Aleksandrowicz E, Lysiak-Szydlowska W, Rutkowski B. (2008) Triple pharmacological blockade of the renin-angiotensin-aldosterone system in non-diabetic CKD: an open-label crossover randomized controlled trial. *Am J Kidney Dis* 52: 486-493.

Van den Akker E, Satchwell TJ, Williamson RC, Toye AM. (2010) Band 3 multiprotein complexes in the red cell membrane; of mice and men. *Blood Cells Mol Dis* 45(1): 1-8.

Verpoorte, JA, Mehta S, Edsall, JT. (1967) Esterase activities of human carbonic anhydrases B and C. *J Biol Chem* 242: 4221–4229.

Viengchareun S, Le Menuet D, Martinerie L, Munier M, Pascual-LeTallec L, Lombes M. (2007) The mineralocorticoid receptor: insights into its molecular and (patho)physiological biology. *Nucl Recept Signal* 5: e012.

Walton KM, Dixon JE. (1993) Protein tyrosine phosphatases. *Annu Rev Biochem* 62: 101-120.

Wang DN. (1994) Band 3 protein: structure, flexibility and function. *FEBS Lett* 346(1): 26-31.

Weiwei Z, Hu R. (2009) Targeting carbonic anhydrase to treat diabetic retinopathy: emerging evidences and encouraging results. *Biochem Biophys Res Commun* 390: 368-371.

Xu W, Harrison SC, Eck MJ. (1997) Three-dimensional structure of the tyrosine kinase c-Src. *Nature* 385: 595-602.

Yamaji M, Tsutamoto T, Kawahara C, Nishiyama K, Yamamoto T, Fujii M, Horie M. (2009) Serum cortisol as a useful predictor of cardiac events in patients with chronic heart failure: the impact of oxidative stress. *Circ Heart Fail* 2: 608-615.

Yang J, Chang CY, Safi R, Morgan J, McDonnell DP, Fuller PJ, Clyne CD, Young MJ. (2011) Identification of ligand-selective peptide antagonists of the mineralocorticoid receptor using phage display. *Mol Endocrinol* 25: 32-43.

Yang J, Fuller PJ. (2012) Interactions of the mineralocorticoid receptor-within and without. *Mol Cell Endocrinol* 350: 196-205.

Yannoukakos D, Vasseur C, Piau JP, Wajcman H, Bursaux E. (1991) Phosphorylation sites in human erythrocyte band 3 protein. *Biochim Biophys Acta* 1061: 253-266.

Yazdanbakhsh K, Lomas-Francis C, Reid ME. (2000) Blood groups and diseases associated with inherited abnormalities of the red blood cell membrane. *Transfus Med Rev* 14 (4): 364–374.

Zennaro MC, Boulkroun S, Fernandes-Rosa F. (2014) An update on novel mechanisms of primary aldosteronism. *J Endocrinol* 224(2): R63-R77.

Zonta F, Pagano MA, Trentin L, Tibaldi E, Frezzato F, Gattazzo C, Martini V, Trimarco V, Mazzorana M, Bordin L, Semenzato G, Brunati AM. (2014) Lyn-mediated procaspase 8 dimerization blocks apoptotic signaling in B-cell chronic lymphocytic leukemia. *Blood* 123: 875-883.

Other studies carried out during PhD program

During my PhD I also collaborated with Professor Decio Armanini and his working group at Department of Medicine – Endocrinology (University of Padova), participating in various projects.
The oxidization processes, at the basis of my investigations, and their biological impacts were also evaluated in RBC from patients with other inflammatory diseases (polycystic ovary syndrome and endometriosis) and in other cells (spermatozoa).

PCOs and Endometriosis

Polycystic ovary syndrome (PCOs) and endometriosis are two different pathologies which I demonstrated to share a common denominator: an oxidative-related increase in glutathionylation of membrane proteins with an enhanced band 3 aggregates and Tyr-phosphorylation process (Donà et al., 2012; Andrisani et al., 2014).

Spermatozoa

I began sperm investigations before my PhD training and occasionally I addressed again to better comprehend the involvement of ROS and oxidative assault in the membrane alterations and Tyr-phosphorylation.
By the time-dependent evaluation of sperm ROS production as a simple method for rapid clinical estimation of the fertilizing ability of these cells, I evaluated different commercial buffers commonly used to induce sperm capacitation. This process, strictly related to membrane alterations and Tyr-phosphorylation of sperm head, would predispose sperm to the best conditions for the following intrauterine insemination (IUI) or in vitro fecundation (IVF), by far increasing reproductive success. After reporting what was the best medium for capacitating the highest number of cells and preventing time-dependent apoptosis (Andrisani et al., 2014), I investigated potential effectors able to ameliorate patients' sperm by regulating endogenous ROS productions. I found that astaxanthin (Asta), a photo-

protective red pigment synthesized by the microalgae and belonging to the carotenoid family, was able to perturb sperm membrane organization by inserting into the membrane bilayer without altering/scavenging superoxides. In this way, Asta may set free proteins involved in the following Tyr-phosphorylation process and related acrosome reaction, even in the absence of additional stimuli, such as ROS lipid peroxidation (Donà et al., 2013).

Data were published in:

Andrisani A, **Donà G***, Brunati AM, Clari G, Armanini D, Ragazzi E, Ambrosini G, Bordin L. (2014) Increased oxidation-related glutathionylation and carbonic anhydrase activity in endometriosis. *Reprod Biomed Online* 28(6): 773-779.

*** Authors A. Andrisani and G. Donà contributed equally**

Andrisani A, **Donà G***, Ambrosini G, Bonanni G, Bragadin M, Cosmi E, Clari G, Armanini D, Bordin L. (2014) Effect of various commercial buffers on sperm viability and capacitation. *Syst Biol Reprod Med* 60(4): 239-244.

*** Corresponding author**

Armanini D, Sabbadin C, **Donà G**, Clari G, Bordin L. (2014) Aldosterone receptor blockers spironolactone and canrenone: two multivalent drugs. *Expert Opin Pharmacother* 15(7): 909-912.

Armanini D, Ambrosini G, Sabbadin C, **Donà G**, Clari G, Bordin L. (2013) Microalbuminuria and hypertension in pregnancy: role of aldosterone and inflammation. *J Clin Hypertens (Greenwich)* 15(9): 612-614.

Donà G, Kožuh I, Brunati AM, Andrisani A, Ambrosini G, Bonanni G, Ragazzi E, Armanini D, Clari G, Bordin L. (2013) Effect of astaxanthin on human sperm capacitation. *Mar Drugs* 11(6): 1909-1919.

Bordin L, **Donà G**, Sabbadin C, Ragazzi E, Andrisani A, Ambrosini G, Brunati AM, Clari G, Armanini D. (2013) Human red blood cells alterations in primary aldosteronism. *J Clin Endocrinol Metab* 98(6): 2494-2501.

Armanini D, Bordin L, **Donà G**, Sabbadin C, Bakdounes L, Ragazzi E, Giorgino FL, Fiore C. (2012) Polycystic ovary syndrome: Implications of measurement of plasma aldosterone, renin activity and progesterone. *Steroids* 77(6): 655-658.

Donà G, Sabbadin C, Fiore C, Bragadin M, Giorgino FL, Ragazzi E, Clari G, Bordin L, Armanini D. (2012) Inositol administration reduces oxidative stress in erythrocytes of patients with polycystic ovary syndrome. *Eur J Endocrinol* 166(4): 703-710.

Aknwoledgments

Questa tesi di dottorato è la conclusione di tre anni ricchi ed intensi, dedicati a questa esperienza di ricerca, segnata purtroppo da momenti difficili ma anche da tante soddisfazioni. Vorrei ringraziare tutte le persone che, sia nell'ambito lavorativo che in quello familiare, hanno contribuito al raggiungimento di questo importante obiettivo.

Vorrei ringraziare il Prof. Ursini per essere subentrato come tutor, permettendomi di concludere il dottorato.

Un ringraziamento e un affettuoso ricordo va al Prof. Giulio Clari, che mi ha permesso di intraprendere questa esperienza di ricerca nel suo laboratorio e che tanto ha saputo trasmettermi sia nell'ambito lavorativo che dal punto di vista umano.

Un immenso ringraziamento va alla Dott.sa Luciana Bordin, persona speciale, amica e collega. Ha saputo insegnarmi molto sul mondo della ricerca con competenza ed entusiasmo, facendomi appassionare ai nostri progetti e condividendo con me le difficoltà di questi anni, ma anche gioie e soddisfazioni.

Ringrazio il Prof. Decio Armanini per la collaborazione, la presenza sempre attenta e la fiducia ed il sostegno che ha sempre dimostrato.

Un caro ringraziamento anche le amiche Francesca, Elena e Chiara per la collaborazione, la compagnia, le chiacchiere e per aver condiviso con me questo percorso.

Ed infine un ringraziamento speciale va a Stefano ed ai miei genitori, Rosanna e Giovanni, che con grande pazienza hanno saputo supportarmi ed accompagnarmi in questi anni, facendomi sentire sempre il loro sostegno.